LEGENDRE WAVELET COLLOCATION METHOD WITH QUASILINEARIZATION TECHNIQUE FOR FRACTIONAL DIFFERENTIAL EQUATIONS

A Thesis Submitted to
the Graduate School of Engineering and Sciences of
İzmir Institute of Technology
in Partial Fulfillment of the Requirements for the Degree of

MASTER OF SCIENCE

in Mathematics

by
Fatih İDİZ

December 2022
İZMİR

ACKNOWLEDGMENTS

First of all, I would like to thank my advisor, Prof. Dr. Gamze Tanoğlu. I feel very lucky that she is my advisor. Whenever I needed to talk to her, she always tried to arrange a meeting, even if she didn't have free time.

I am extremely grateful to Prof. Dr. Nasser Aghazadeh and Dr. Amir Mohammadi. I am glad our paths crossed. They made a great contribution to my thesis. They answered all my questions and proofread my thesis.

I would like to thank my neighbors in Izmir, Ms. Yıldız Çümen, Mr. Mehmet Asım Çümen, Ms. Kamile Sarmaşık, and Mr. Savaş Sarmaşık. Thanks to the Çümen family and the Sarmaşık family, I had a joyful time during my stay in Izmir. They treated me like family.

I would like to acknowledge the scholarship awarded by the Scientific and Technological Research Institution of Turkey (TUBITAK) within the scope of "2210-National Scholarship Program for M.Sc. Students".

Many people made contributions to the preparation of this thesis. If I haven't mentioned their names, it's not because I underestimated their help, but because I forgot to thank them.

ABSTRACT

LEGENDRE WAVELET COLLOCATION METHOD WITH QUASILINEARIZATION TECHNIQUE FOR FRACTIONAL DIFFERENTIAL EQUATIONS

We aim to present numerical methods based on Legendre wavelets and quasilinearization technique for fractional Lane-Emden type equations and time-fractional Fisher's equation.

The Lane-Emden equation is a second order singular non-linear ordinary differential equation, which is useful for modelling many astrophysical phenomena such as the distribution of stars in star clusters and star formation in molecular clouds. The Fisher's equation is a non-linear reaction-diffusion equation that models the spread of mutant genes in a population.

We start with a brief discussion of the purpose of studying fractional differential equations. Then some practical aspects of wavelets are explained. We also give introductory definitions and properties of fractional calculus and Legendre wavelets. Using Legendre wavelets and quasilinearization technique, we derive numerical methods for fractional Lane-Emden type equations and time-fractional Fisher's equation. Moreover, the convergence analysis of both methods is studied. Some problems are solved to evaluate the efficiency of the proposed methods. Test problems show that the proposed methods are very effective.

ÖZET

KESİRLİ DİFERANSİYEL DENKLEMLER İÇİN KUASİLİNEERİZASYON TEKNİĞİ İLE LEGENDRE DALGACIĞI KOLLOKASYON METODU

Kesirli Lane-Emden tipi denklemler ve zaman-kesirli Fisher denklemi için Legendre dalgacıklarına ve kuasilineerizasyon tekniğine dayalı nümerik yöntemler sunmayı amaçlıyoruz.

Lane-Emden denklemi, yıldız kümelerindeki yıldızların dağılımı ve moleküler bulutlardaki yıldız oluşumu gibi birçok astrofiziksel olguyu modellemek için yararlı olan ikinci dereceden tekil, doğrusal olmayan bir adi diferansiyel denklemdir. Fisher denklemi ise, bir popülasyondaki mutant genlerin yayılmasını modelleyen doğrusal olmayan bir reaksiyon-difüzyon denklemidir.

Kesirli diferansiyel denklemleri çalışmanın amacına ilişkin kısa bir tartışma ile başlıyoruz. Daha sonra dalgacıkların bazı pratik yönleri açıklanmaktadır. Ayrıca kesirli kalkülüs ve Legendre dalgacıklarının giriş seviyesi tanımları ve özellikleri verilmektedir. Legendre dalgacıklarını ve kuasilineerizasyon tekniğini kullanarak, kesirli Lane-Emden tipi denklemler ve zaman-kesirli Fisher denklemi için nümerik yöntemler elde edilmiştir. Ayrıca, her iki yöntemin yakınsama analizi incelenmiştir. Önerilen yöntemlerin etkinliğini değerlendirmek için bazı problemler çözülmüştür. Test problemleri, önerilen yöntemlerin çok etkili olduğunu göstermektedir.

TABLE OF CONTENTS

LIST OF FIGURES vi

LIST OF TABLES viii

CHAPTER 1. INTRODUCTION 1

CHAPTER 2. PRELIMINARIES 6
2.1. Fractional Calculus 6
2.2. Wavelets 7
2.2.1. Legendre Polynomials and Legendre Wavelets 8

CHAPTER 3. FRACTIONAL LANE-EMDEN TYPE EQUATIONS 19
3.1. Quasilinearization 19
3.2. Description of the Proposed Method 21
3.3. Convergence Analysis 22
3.4. Numerical Examples 23

CHAPTER 4. TIME-FRACTIONAL FISHER'S EQUATION 36
4.1. Quasilinearization 36
4.2. Description of the Proposed Method 38
4.3. Convergence Analysis 42
4.4. Numerical Examples 45

CHAPTER 5. CONCLUSION 55

REFERENCES 56

LIST OF FIGURES

Figure **Page**

Figure 3.1 The graphs of numerical solutions for various pairs of α and β in Example 3.1.a obtained by LWCMQT with $b = 3$ and $D = 8$. 25

Figure 3.2 Exact solution and approximate solution of Example 3.1.a for $\alpha = 2$, $\beta = 1$ and $b = 2$, $D = 8$ obtained by LWCMQT. 25

Figure 3.3 Absolute error $|y_{exact}(r) - y_{approximate}(r)|$ in Example 3.1.a for $\alpha = 2$, $\beta = 1$ and $b = 2$, $D = 8$. 26

Figure 3.4 The graphs of numerical solutions for various pairs of α and β in Example 3.1.b obtained by LWCMQT with $b = 3$ and $D = 8$ in the third iteration. 27

Figure 3.5 For $\alpha = 2$ and $\beta = 1$, the plot of the exact solution along with the plots of numerical solutions in the first, second, and third iteration in Example 3.1.b obtained by LWCMQT with $b = 3$ and $D = 8$ 28

Figure 3.6 For $\alpha = 2$, $\beta = 1$, and $b = 3$, $D = 8$, the graphs of absolute errors in Example 3.1.b 30

Figure 3.7 Numerical solutions for various pairs of α and β in Example 3.2 obtained by LWCMQT with $b = 3$ and $D = 8$ in the third iteration. . . 32

Figure 3.8 For $\alpha = 2$ and $\beta = 1$, the plot of the exact solution along with the plots of numerical solutions in the first, second, and third iteration in Example 3.2 obtained by LWCMQT with $b = 3$ and $D = 8$ 32

Figure 3.9 For $\alpha = 2$, $\beta = 1$, and $b = 3$, $D = 8$, the graphs of absolute errors in Example 3.2 33

Figure 3.10 Numerical solutions for various pairs of α and β in Example 3.3 obtained by LWCMQT with $b = 3$ and $D = 8$ in the third iteration. . . 34

Figure 3.11 For $\alpha = 2$ and $\beta = 1$, the plot of the exact solution along with the plots of numerical solutions in the first, second, and third iteration in Example 3.3 obtained by LWCMQT with $b = 3$ and $D = 8$ 34

Figure 3.12 For $\alpha = 2$, $\beta = 1$, and $b = 3$, $D = 8$, the graphs of absolute errors in Example 3.3 35

Figure 4.1 Numerical solution for $\alpha = 1$ obtained by LWCMQT with $b = 2$, $h = 2$ and $D = 2$, $Q = 2$ in the 3^{rd} iteration in Example 4.1 46

Figure 4.2 The absolute error $|y_{exact}(x,t) - y_3(x,t)|$ of Example 4.1 48

Figure 4.3 Numerical solution for $\mu = \frac{2}{3}$ and $\alpha = 1$ obtained by LWCMQT with $b = 2$, $h = 2$ and $D = 2$, $Q = 2$ in the 3^{rd} iteration in Example 4.2 . . 49

Figure **Page**

Figure 4.4 The absolute error $|y_{exact}(x,t) - y_3(x,t)|$ of Example 4.2 51
Figure 4.5 Numerical solution for $\alpha = 1$ obtained by LWCMQT with $b = 2$, $h = 2$ and $D = 2$, $Q = 2$ in the 3^{rd} iteration in Example 4.3 52
Figure 4.6 The absolute error $|y_{exact}(x,t) - y_3(x,t)|$ of Example 4.3 54

LIST OF TABLES

Table **Page**

Table 3.1 Maximum absolute errors (E_{L_∞}) for $\alpha = 2$ and $\beta = 1$ obtained by various numerical methods in Example 3.1.a 24

Table 3.2 Maximum absolute errors (E_{L_∞}) for $\alpha = 2$ and $\beta = 1$ obtained by various numerical methods in Example 3.1.b 26

Table 3.3 Numerical results for $\alpha = 2$, $\beta = 1$ and $b = 2$, $D = 8$ in Example 3.2 obtained by ADM, HWCM, CWCQM, and LWCMQT in the third iteration. 31

Table 3.4 Maximum absolute errors (E_{L_∞}) for $\alpha = 2$ and $\beta = 1$ obtained by various numerical methods in Example 3.3 32

Table 4.1 Numerical results for Example 4.1 obtained by using the LWCMQT with the resolution levels $b = 2$, $h = 2$ and the degree of polynomials $D = 2$, $Q = 2$ 47

Table 4.2 Maximum absolute errors (E_{L_∞}) of LWCMQT, HWCIM [2], and MVIM [28] for the numerical solution of Example 4.1 47

Table 4.3 Numerical results for Example 4.2 obtained by using the LWCMQT with the resolution levels $b = 2$, $h = 2$ and the degree of polynomials $D = 2$, $Q = 2$ 50

Table 4.4 Maximum absolute errors (E_{L_∞}) of LWCMQT, HWCIM [2], and MVIM [28] for the numerical solution of Example 4.2 50

Table 4.5 Numerical results for Example 4.3 obtained by using the Legendre wavelet collocation method with quasilinearization technique with the resolution levels $b = 2$, $h = 2$ and the degree of polynomials $D = 2$, $Q = 2$ 53

Table 4.6 Maximum absolute errors (E_{L_∞}) of LWCMQT, and HWCIM [2] for the numerical solution of Example 4.3 53

CHAPTER 1

INTRODUCTION

The subject of fractional calculus is roughly derivatives and integrals, whose order can be real or complex numbers. However, the term *"fractional"* is a historical misnomer because in fractional calculus the order of derivatives and integrals need not be fractional(rational) numbers.

The first appearance of fractional calculus is in a letter between L'Hopital and Leibniz in 1695. Leibniz asked L'Hopital

"*Is it possible to extend the concept of the integer order derivative* $\frac{d^n y}{dx^n}$ *to be meaningful when the order* n *is a fraction?*"

L'Hopital replied

"*What happens if the order* n *is* $\frac{1}{2}$*?*"

Based on the mathematics of his own time, Leibniz responded that

"*When* n *is* $\frac{1}{2}$*, it will result in a paradox that will one day yield beneficial and practical results.*"

Leibniz and L'Hopital were not the only mathematicians interested in fractional calculus. Numerous prominent mathematicians were interested in fractional calculus, including Euler, Riemann, Liouville, Abel, and Laplace.

Until the 20th century, fractional calculus was studied by pure mathematicians. Recently, it is found that many real life problems are modelled better using fractional differential equations [3], [15], [22], [29], [9]. There are two main reasons for this: First of all, we don't have to use only integer order derivatives and integrals; we are allowed to use any order for the integral and derivative operators. Second, fractional derivative operator is not a local operator. This means that if we interpret the independent variable as time, the fractional derivative of a function depends also on the past data of the function, which can be easily realized from the definition of the Caputo fractional derivative in

Chapter 2. This property helps us more accurately model problems with memory, such as the SIR model in epidemics [8]. Furthermore, there are mathematical models that can only be described using fractional differential equations. For example, the Bagley-Torvik equation is used to describe how a rigid plate moves when submerged in a Newtonian fluid, and it involves a fractional order differential term [38]. For these reasons, fractional calculus has become attractive to many scientists and engineers.

Unfortunately, it is not always possible to find an exact solution to a fractional differential equation. Hence, many researchers develop numerical methods to find approximate solutions. Some of the most commonly used numerical methods are Variational Iteration Method (VIM) [7], Adomian Decomposition Method (ADM) [17], Homotopy Perturbation Method (HPM) [40], and Finite Difference Method (FDM) [21]. Also, spectral methods such as collocation [36], [45] and Galerkin methods [14], [20] are popular among other numerical methods for solving fractional differential equations because of their fast convergence properties.

Wavelet theory has been developed and applied to various research fields over the past three decades. Wavelets are employed to solve problems in economics [25], signal processing [37], inverse problems [26], etc. A Schauder basis for the space of square-integrable functions on the interval $[a, b]$ can be constructed using appropriately scaled and shifted wavelets. Thus, we can express any function $f \in L^2[a, b]$ in terms of wavelets. Based on this property, numerous scholars have proposed numerical methods for solving fractional differential equations [10], [43], [39], [41], [1]. By taking advantage of this feature, we are going to propose numerical methods which depend on Legendre wavelets and quasilinearization technique.

Many real life problems in science and engineering can be modelled using ordinary differential equations and partial differential equations. The Lane-Emden equation can be given as an example for ordinary differential equations. And the Fisher's equation can be given as an example of partial differential equations.

The Lane-Emden equation usually appears in astrophysics and is given by

$$y''(r) + \frac{2}{r}y'(r) + y^m(r) = 0, \qquad r > 0. \tag{1.1}$$

depending on the initial conditions

$$y(0) = P, \qquad y'(0) = Q, \tag{1.2}$$

where $m, P, Q \in \mathbb{R}$ are constants. The Lane-Emden equation (1.1) is useful to model the internal structure of a ball of gas or plasma under self-gravitation, the distribution of stars in star clusters under self-gravitation, star formation in molecular clouds, and the theory of thermionic currents [6]. The Lane-Emden equation (1.1) was first studied by Jonathan Homer Lane in 1870. 37 years later, in 1907, the equation (1.1) was investigated in more detail by Robert Emden.

In this study, we consider the following form of fractional Lane-Emden type of equations

$$\frac{d^\alpha y(r)}{dr^\alpha} + \frac{K}{r^{\alpha-\beta}} \frac{d^\beta y(r)}{dr^\beta} + h(r, y(r)) = 0, \qquad r > 0, \tag{1.3}$$

with the initial conditions

$$y(0) = P, \qquad y'(0) = Q, \tag{1.4}$$

where $K, P, Q \in \mathbb{R}$ are constants. r is the independent variable and y is the dependent variable. $h(r, y(r))$ represents a nonlinear function of r and $y(r)$. $\frac{d^\alpha y(r)}{dr^\alpha}$ and $\frac{d^\beta y(r)}{dr^\beta}$ denote the α-th and β-th order Caputo fractional derivative of $y = y(r)$, where $1 < \alpha \leq 2$ and $0 < \beta \leq 1$, respectively. The existence and uniqueness of the solutions to the problem (1.3) with (1.4) is studied in [12]. Due to the term $\frac{K}{r^{\alpha-\beta}}$, equation (1.3) is a singular initial value problem. Lane-Emden type equations are challenging to solve numerically because of the presence of singularity at $r = 0$. By choosing an appropriate α, β, K, and h, the Lane-Emden type equation (1.3) can be reduced to the Thomas-Fermi equation or the Poisson-Boltzmann-Emden equation. So, the Lane-Emden type equation (1.3) is a generalization of the classical Lane-Emden equation (1.1), Thomas-Fermi equation, and Poisson-Boltzmann-Emden equation.

There exist various methods to find an approximate solution to fractional Lane-Emden type equations (1.3). Amir Mohammadi *et al.* [27] used second-kind Chebyshev wavelet method together with quasilinearization technique to solve fractional Lane-Emden type equations. Umer Saeed [32] proposed a numerical method based on Haar wavelets and Adomian decomposition method. For the classical Lane-Emden equation (1.1), there are also many other numerical methods in the literature [13], [30], [35].

In addition to the fractional Lane-Emden type equation (1.3), we consider the following form of the time-fractional Fisher's equation

$$\frac{\partial^\alpha y(x,t)}{\partial t^\alpha} = \delta \frac{\partial^2 y(x,t)}{\partial x^2} + \lambda y(x,t)(1 - y^p(x,t)) + q(x,t) \tag{1.5}$$

$$0 \leq x \leq 1, \qquad 0 \leq t \leq 1.$$

The initial condition is

$$y(x,0) = w(x), \tag{1.6}$$

and boundary conditions are

$$y(0,t) = z_1(t), \tag{1.7}$$

$$y(1,t) = z_2(t), \tag{1.8}$$

where $\delta, \lambda, p \in \mathbb{R}$; $w(x)$, $z_1(t)$, $z_2(t)$, and $q(x,t)$ are known functions. $\dfrac{\partial^\alpha y(x,t)}{\partial t^\alpha}$ denotes the α-th order Caputo fractional derivative of $y = y(x,t)$ with respect to t, where $0 < \alpha \leq 1$. In 1937, Fisher proposed the following simplified form of equation (1.5) to investigate how a mutant gene spreads in a population; where y represents the density of the mutant gene in the population [11].

$$\frac{\partial y(x,t)}{\partial t} = \delta \frac{\partial^2 y(x,t)}{\partial x^2} + \lambda y(x,t)(1 - y(x,t)). \tag{1.9}$$

The Fisher's equation is also used in many areas of science and engineering such as chemical kinetics [31], branching Brownian motion [5], epidemics and bacteria [19].

Aghazadeh *et al.* [2] used Haar wavelet method together with Picard iteration to solve the time-fractional Fisher's equation numerically. Mohyud-Din *et al.* [28] obtained numerical results for the Fisher's equation using the modified variational iteration method. Secer *et al.* [33] developed a computational approach for the time-fractional Fisher's equation based on Jacobi wavelets.

CHAPTER 2

PRELIMINARIES

The main goal of this chapter is to present the fundamentals of fractional calculus and Legendre wavelets.

2.1 Fractional Calculus

Definition 1. [18] Let $\alpha \in \mathbb{R}^+$ and $\Omega = [a, b]$ be a finite interval, where $-\infty < a < b < \infty$. For a function $u \in L^1[a, b]$, its Riemann-Liouville integral of order α is defined by

$$ {}_a\mathcal{I}_t^{\alpha} u(t) = \frac{1}{\Gamma(\alpha)} \int_a^t (t - x)^{\alpha - 1} u(x)\, dx, \tag{2.1} $$

where Γ denotes the gamma function and $t \in [a, b]$. For $\alpha = 0$, we set

$$ {}_a\mathcal{I}_t^{0} u(t) = u(t). \tag{2.2} $$

Useful properties for the Riemann-Liouville integral operator [18]:

1. Consider the function $u(t) = (t - a)^{\lambda}$ with $\lambda > -1$. For $\alpha \in \mathbb{R}^+$, we have

$$ {}_a\mathcal{I}_t^{\alpha} u(t) = \frac{\Gamma(\lambda + 1)}{\Gamma(\lambda + \alpha + 1)} (t - a)^{\lambda + \alpha}. \tag{2.3} $$

2. Let $\alpha, \beta \in \mathbb{R}^+$. Suppose that u is an absolutely integrable function over $[a, b]$, i.e., $u \in L^1[a, b]$. Then there holds

$$ {}_a\mathcal{I}_t^{\alpha}\, {}_a\mathcal{I}_t^{\beta} u(t) = {}_a\mathcal{I}_t^{\beta}\, {}_a\mathcal{I}_t^{\alpha} u(t) = {}_a\mathcal{I}_t^{\alpha + \beta} u(t). \tag{2.4} $$

Definition 2. [18] Let $\alpha \in \mathbb{R}^+$ and $\Omega = [a, b]$ be a finite interval, where $-\infty < a < b < \infty$. For a function $u \in L^1[a, b]$, its Caputo derivative of order α is defined by

$$ {}_a^C\mathcal{D}_t^\alpha u(t) = \begin{cases} \dfrac{1}{\Gamma(n-\alpha)} \displaystyle\int_a^t (t-x)^{n-\alpha-1} u^{(n)}(x)\, dx, & n-1 < \alpha < n,\ n \in \mathbb{N}; \\ \dfrac{d^n}{dt^n} u(t), & \alpha = n,\ n \in \mathbb{N}, \end{cases} \tag{2.5} $$

where Γ represents the gamma function and $t \in [a, b]$.

We have the following relations between the Riemann-Liouville fractional integral and the Caputo fractional derivative [18]:

1. Let $\alpha \in \mathbb{R}^+$ such that $n - 1 < \alpha < n$, where $n \in \mathbb{N}$. Suppose that $u \in C[a, b]$. Then

$$ {}_a^C\mathcal{D}_t^\alpha \, {}_a\mathcal{I}_t^\alpha u(t) = u(t), \tag{2.6} $$

   for all $t \in [a, b]$.

2. Let $\alpha \in \mathbb{R}^+$ such that $n - 1 < \alpha < n$, where $n \in \mathbb{N}$. If $u \in C^n[a, b]$, then

$$ {}_a\mathcal{I}_t^\alpha \, {}_a^C\mathcal{D}_t^\alpha u(t) = u(t) - \sum_{k=0}^{n-1} u^{(k)}(a) \frac{(t-a)^k}{k!}, \tag{2.7} $$

   for all $t \in [a, b]$.

2.2 Wavelets

Wavelets are a special kind of family of functions. The family of functions is created by scaling and shifting a single function, known as the mother wavelet. Each wavelet function in the family can be described using the mother wavelet, the scaling parameter p, and the shifting parameter r as follows:

$$ \psi_{p,r}(t) = |p|^{-1/2} \psi\left(\frac{t-r}{p}\right), \quad p, r \in \mathbb{R}, \quad p \neq 0. \tag{2.8} $$

By restricting the scaling parameter p and shifting parameter r to $p = p_0^{-k}$ and $r = nr_0p_0^{-k}$, where $p_0 > 1$, $r_0 > 0$, and $k, n \in \mathbb{Z}$; we get a countable set of wavelets Ψ whose members are of the form

$$\psi_{k,n}(t) = {p_0}^{k/2}\psi({p_0}^k t - nr_0). \tag{2.9}$$

The countable set of wavelets $\Psi = \{\psi_{k,n} : k, n \in \mathbb{Z}\}$ forms a Schauder basis for the Hilbert space $L^2(\mathbb{R})$.

2.2.1 Legendre Polynomials and Legendre Wavelets

The Legendre polynomials are a special collection of orthogonal polynomials on the interval $[-1, 1]$. The d-th degree Legendre polynomial can be determined using the recursion formula

$$L_0(t) = 1, \qquad L_1(t) = t, \tag{2.10}$$

$$(d+1)L_{d+1}(t) = (2d+1)tL_d(t) - dL_{d-1}(t), \qquad d = 1, 2, 3, \ldots . \tag{2.11}$$

The Legendre polynomials are orthogonal with respect to the weight function $w(t) = 1$ on $[-1, 1]$. More precisely, we have

$$\langle L_d, L_g\rangle_2 = \int_{-1}^{1} L_d(t)L_g(t)\,dt = \begin{cases} \dfrac{2}{2d+1}, & d = g; \\ 0, & \text{otherwise.} \end{cases} \tag{2.12}$$

An explicit formula for the Legendre polynomials is given by

$$L_d(t) = \sum_{g=0}^{d} \binom{d}{g}\binom{d+g}{g}\left(\frac{t-1}{2}\right)^g. \tag{2.13}$$

For practical use of polynomials on the interval $[0, 1]$, the shifted Legendre polynomials on the interval $[0, 1]$ can be expressed as

$$G_d(t) = L_d(2t - 1),$$

where L_d represents the d-th degree Legendre polynomial.

Legendre wavelets $\psi_{c,d}(t) = \psi(b, c, d, t)$ consist of Legendre polynomials and have four parameters. Legendre wavelets can be described on the interval $[0, 1)$ as follows:

$$\psi_{c,d}(t) = \begin{cases} \sqrt{\frac{2d+1}{2}} 2^{b/2} L_d(2^b t - 2c + 1), & \frac{2c-2}{2^b} \leq t < \frac{2c}{2^b}; \\ 0, & \text{otherwise.} \end{cases} \tag{2.14}$$

Here, b is the resolution level and it can be any positive integer. c can take the values $c = 1, 2, \ldots, 2^{b-1}$. d represents the degree of Legendre polynomials and it can be $d = 0, 1, \ldots, D - 1$, where $D \in \mathbb{Z}^+$ is a fixed number. The term $\left(\frac{2d+1}{2}\right)^{1/2}$ is required for orthonormality. The scaling parameter is $p = 2^{-b}$ and the shifting parameter is $r = (2c - 1)2^{-b}$. L_d denotes the d-th degree Legendre polynomials defined on $[-1, 1]$. It should be noted that

$$\langle \psi_{c_1,d_1}, \psi_{c_2,d_2} \rangle_2 = \int_0^1 \psi_{c_1,d_1}(t) \psi_{c_2,d_2}(t)\, dt = \begin{cases} 1, & c_1 = c_2 \text{ and } d_1 = d_2; \\ 0, & \text{otherwise.} \end{cases} \tag{2.15}$$

Equaivalently, Legendre wavelets can be defined using the shifted Legendre polynomials as follows:

$$\psi_{c,d}(t) = \begin{cases} \sqrt{\frac{2d+1}{2}} 2^{b/2} G_d(2^{b-1} t - c + 1), & \frac{2c-2}{2^b} \leq t < \frac{2c}{2^b}; \\ 0, & \text{otherwise.} \end{cases} \tag{2.16}$$

Any function $y(t) \in L^2([0, 1))$ can be expressed in terms of Legendre wavelets as

follows:

$$y(r) = \sum_{c=1}^{\infty} \sum_{d=0}^{\infty} a_{c,d} \psi_{c,d}(r), \tag{2.17}$$

where

$$a_{c,d} = \langle y(r), \psi_{c,d}(r) \rangle \tag{2.18}$$

$$= \int_0^1 y(r) \psi_{c,d}(r)\, dr. \tag{2.19}$$

If we truncate the infinite series (2.17), we can approximate $y(r)$

$$y(r) \approx y_{b,D}(r) = \sum_{c=1}^{2^{b-1}} \sum_{d=0}^{D-1} a_{c,d} \psi_{c,d}(r), \tag{2.20}$$

where $b, D \in \mathbb{Z}^+$. If we change the indices c, d by $i = D(c-1) + d + 1$, we can rewrite approximation (2.20) as

$$y(r) \approx y_{b,D}(r) = \sum_{i=1}^{2^{b-1}D} a_i \psi_i(r). \tag{2.21}$$

Using Legendre wavelets, any function $y(x,t) \in L^2([0,1) \times [0,1))$ may be written as follows:

$$y(x,t) = \sum_{c=1}^{\infty} \sum_{d=0}^{\infty} \sum_{p=1}^{\infty} \sum_{q=0}^{\infty} a_{c,d,p,q} \psi_{c,d}(x) \psi_{p,q}(t), \tag{2.22}$$

where

$$a_{c,d,p,q} = \langle \psi_{c,d}(x), \langle y(x,t), \psi_{p,q}(t) \rangle \rangle \tag{2.23}$$

$$= \int_0^1 \int_0^1 y(x,t)\psi_{c,d}(x)\psi_{p,q}(t)\, dx\, dt. \tag{2.24}$$

If we truncate the infinite series (2.22), we can approximate $y(x,t)$

$$y(x,t) \approx y_{b,D,h,Q}(x,t) = \sum_{c=1}^{2^{b-1}} \sum_{d=0}^{D-1} \sum_{p=1}^{2^{h-1}} \sum_{q=0}^{Q-1} a_{c,d,p,q}\psi_{c,d}(x)\psi_{p,q}(t), \tag{2.25}$$

where $b, h, D, Q \in \mathbb{Z}^+$. If we change the indices c, d and p, q by $i = D(c-1) + d + 1$ and $j = Q(p-1) + q + 1$, respectively; we can rewrite approximation (2.25) as

$$y(x,t) \approx y_{b,D,h,Q}(x,t) = \sum_{i=1}^{2^{b-1}D} \sum_{j=1}^{2^{h-1}Q} a_{i,j}\psi_i(x)\psi_j(t). \tag{2.26}$$

We need to find the Riemann-Liouville integral of Legendre wavelets to implement the numerical methods that will be introduced in the next chapters. Almost all numerical methods are difficult to implement using pen and paper. For this reason, we use computers to implement numerical methods. However, calculating an integral on a computer can be quite time-consuming. Therefore, we are going to propose a formula to calculate the Riemann-Liouville integral of Legendre wavelets. In our formula, the Riemann-Liouville integral of Legendre wavelets can be calculated using finite sums. And this makes the calculation of the Riemann-Liouville integral of Legendre wavelets on a computer considerably fast.

Theorem 1. For any Legendre wavelet $\psi_{c,d}(t)$ on the interval $[0,1)$, its Riemann-Liouville integral of order α can be calculated by

$$
{}_0\mathcal{I}_t^{\alpha}\psi_{c,d}(t) = \begin{cases} 0, & \text{if} \quad t < \dfrac{2c-2}{2^b}; \\ \sqrt{\dfrac{2d+1}{2}}\,2^{b/2} \\ \times \left[\displaystyle\sum_{g=0}^{d}\sum_{z=0}^{g} \binom{d}{g}\binom{d+g}{g}\binom{g}{z} \right. \\ \times (-1)^{g-z}2^{(b-1)z}\,\Gamma(z+1) \\ \left. \times \dfrac{\left(t-\dfrac{2c-2}{2^b}\right)^{\alpha+z}}{\Gamma(\alpha+z+1)} \right], & \text{if} \quad \dfrac{2c-2}{2^b} \le t < \dfrac{2c}{2^b}; \\ \sqrt{\dfrac{2d+1}{2}}\,2^{b/2} \\ \times \left[\displaystyle\sum_{g=0}^{d}\sum_{z=0}^{g} \binom{d}{g}\binom{d+g}{g}\binom{g}{z} \right. \\ \times (-1)^{g-z}2^{(b-1)z}\,\Gamma(z+1) \\ \times \dfrac{\left(t-\dfrac{2c-2}{2^b}\right)^{\alpha+z}}{\Gamma(\alpha+z+1)} - \displaystyle\sum_{g=0}^{d}\binom{d}{g}\binom{d+g}{g} \\ \left. \times\, 2^{(b-1)g}\,\Gamma(g+1)\dfrac{\left(t-\dfrac{2c}{2^b}\right)^{\alpha+g}}{\Gamma(\alpha+g+1)} \right], & \text{if} \quad \dfrac{2c}{2^b} \le t. \end{cases} \tag{2.27}
$$

Proof. Using the unit step function, we can write Legendre wavelets as follows:

$$\psi_{c,d}(t) = \sqrt{\frac{2d+1}{2}} 2^{b/2} \left(v_{\frac{2c-2}{2^b}}(t) L_d(2^b t - 2c + 1) - v_{\frac{2c}{2^b}}(t) L_d(2^b t - 2c + 1) \right), \tag{2.28}$$

where $v_a(t)$ is the unit step function given by

$$v_a(t) = \begin{cases} 1, & \text{if} \quad t \geq a; \\ 0, & \text{if} \quad t < a. \end{cases} \tag{2.29}$$

We make use of the Laplace transform to get $I^\alpha \psi_{c,d}(t)$. The Laplace transform has the following property

$$\mathcal{L}\left\{v_a(t) f(t)\right\} = e^{-as} \mathcal{L}\{f(t+a)\}. \tag{2.30}$$

Using this property, we can write

$$\mathcal{L}\left\{\psi_{c,d}(t)\right\} = \sqrt{\frac{2d+1}{2}} 2^{b/2} \left[e^{-\frac{2c-2}{2^b}s} \mathcal{L}\left\{ L_d\left(2^b\left(t + \frac{2c-2}{2^b}\right) - 2c + 1\right)\right\} - e^{-\frac{2c}{2^b}s} \mathcal{L}\left\{ L_d\left(2^b\left(t + \frac{2c}{2^b}\right) - 2c + 1\right)\right\}\right] \tag{2.31}$$

$$= \sqrt{\frac{2d+1}{2}} 2^{b/2} \left[e^{-\frac{2c-2}{2^b}s} \mathcal{L}\left\{L_d(2^b t - 1)\right\} - e^{-\frac{2c}{2^b}s} \mathcal{L}\left\{L_d(2^b t + 1)\right\}\right]. \tag{2.32}$$

Now, let us find $L_d(2^b t-1)$ and $L_d(2^b t+1)$ by using equation (2.13)

$$L_d(2^b t-1) = \sum_{g=0}^{d} \binom{d}{g}\binom{d+g}{g}\left(\frac{(2^b t-1)-1}{2}\right)^g \tag{2.33}$$

$$= \sum_{g=0}^{d} \binom{d}{g}\binom{d+g}{g}\left(2^{b-1}t-1\right)^g \tag{2.34}$$

$$= \sum_{g=0}^{d} \binom{d}{g}\binom{d+g}{g}\sum_{z=0}^{g}\binom{g}{z}(-1)^{g-z}2^{(b-1)z}t^z \tag{2.35}$$

$$= \sum_{g=0}^{d}\sum_{z=0}^{g} \binom{d}{g}\binom{d+g}{g}\binom{g}{z}(-1)^{g-z}2^{(b-1)z}t^z. \tag{2.36}$$

Similarly, we have

$$L_d(2^b t+1) = \sum_{g=0}^{d} \binom{d}{g}\binom{d+g}{g}\left(\frac{(2^b t+1)-1}{2}\right)^g \tag{2.37}$$

$$= \sum_{g=0}^{d} \binom{d}{g}\binom{d+g}{g}2^{(b-1)g}t^g. \tag{2.38}$$

By taking the Laplace transform of equation (2.36), we get

$$\mathcal{L}\{L_d(2^b t-1)\} = \mathcal{L}\left\{\sum_{g=0}^{d}\sum_{z=0}^{g} \binom{d}{g}\binom{d+g}{g}\binom{g}{z}(-1)^{g-z}2^{(b-1)z}t^z\right\} \tag{2.39}$$

$$= \sum_{g=0}^{d}\sum_{z=0}^{g} \binom{d}{g}\binom{d+g}{g}\binom{g}{z}(-1)^{g-z}2^{(b-1)z}\mathcal{L}\{t^z\} \tag{2.40}$$

$$= \sum_{g=0}^{d}\sum_{z=0}^{g} \binom{d}{g}\binom{d+g}{g}\binom{g}{z}(-1)^{g-z}2^{(b-1)z}\frac{\Gamma(z+1)}{s^{z+1}}. \tag{2.41}$$

Likewise, we take the Laplace transform of equation (2.38).

$$\mathcal{L}\{L_d(2^b t+1)\} = \mathcal{L}\left\{\sum_{g=0}^{d}\binom{d}{g}\binom{d+g}{g}2^{(b-1)g}t^g\right\} \tag{2.42}$$

$$= \sum_{g=0}^{d}\binom{d}{g}\binom{d+g}{g}2^{(b-1)g}\mathcal{L}\left\{t^g\right\} \tag{2.43}$$

$$= \sum_{g=0}^{d}\binom{d}{g}\binom{d+g}{g}2^{(b-1)g}\frac{\Gamma(g+1)}{s^{g+1}}. \tag{2.44}$$

Substituting equation (2.41) and equation (2.44) into equation (2.32), we obtain

$$\mathcal{L}\left\{\psi_{c,d}(t)\right\} = \sqrt{\frac{2d+1}{2}}2^{b/2}\left[e^{-\frac{2c-2}{2^b}s}\mathcal{L}\left\{L_d(2^b t-1)\right\} - e^{-\frac{2c}{2^b}s}\mathcal{L}\left\{L_d(2^b t+1)\right\}\right] \tag{2.45}$$

$$= \sqrt{\frac{2d+1}{2}}2^{b/2}\left[e^{-\frac{2c-2}{2^b}s}\sum_{g=0}^{d}\sum_{z=0}^{g}\binom{d}{g}\binom{d+g}{g}\binom{g}{z}(-1)^{g-z} \times 2^{(b-1)z}\frac{\Gamma(z+1)}{s^{z+1}} - e^{-\frac{2c}{2^b}s}\sum_{g=0}^{d}\binom{d}{g}\binom{d+g}{g}2^{(b-1)g}\frac{\Gamma(g+1)}{s^{g+1}}\right] \tag{2.46}$$

$$= \sqrt{\frac{2d+1}{2}}2^{b/2}\left[\sum_{g=0}^{d}\sum_{z=0}^{g}\binom{d}{g}\binom{d+g}{g}\binom{g}{z}(-1)^{g-z}2^{(b-1)z} \times \frac{\Gamma(z+1)e^{-\frac{2c-2}{2^b}s}}{s^{z+1}} - \sum_{g=0}^{d}\binom{d}{g}\binom{d+g}{g}2^{(b-1)g}\frac{\Gamma(g+1)e^{-\frac{2c}{2^b}s}}{s^{g+1}}\right] \tag{2.47}$$

For a function $F(t)$, we can write its Riemann-Liouville integral of order α in terms of the convolution operator.

$${}_a\mathcal{I}_t^{\alpha}F(t) = \frac{1}{\Gamma(\alpha)}t^{\alpha-1} * F(t), \tag{2.48}$$

where $*$ represents the convolution of $t^{\alpha-1}$ and $F(t)$. That is,

$$t^{\alpha-1} * F(t) = \int_a^t (t-x)^{\alpha-1} F(x)\, dx. \tag{2.49}$$

Since

$${}_0\mathcal{I}_t^{\alpha}\psi_{c,d}(t) = \frac{t^{\alpha-1}}{\Gamma(\alpha)} * \psi_{c,d}(t), \tag{2.50}$$

we can write

$$\mathcal{L}\left\{{}_0\mathcal{I}_t^{\alpha}\psi_{c,d}(t)\right\} = \mathcal{L}\left\{\frac{t^{\alpha-1}}{\Gamma(\alpha)}\right\}\mathcal{L}\left\{\psi_{c,d}(t)\right\} \tag{2.51}$$

$$= \frac{1}{s^{\alpha}}\mathcal{L}\left\{\psi_{c,d}(t)\right\}. \tag{2.52}$$

By substituting equation (2.47) into equation (2.52), we get

$$\mathcal{L}\left\{{}_0\mathcal{I}_t^{\alpha}\psi_{c,d}(t)\right\} = \frac{1}{s^{\alpha}}\sqrt{\frac{2d+1}{2}}2^{b/2}\left[\sum_{g=0}^{d}\sum_{z=0}^{g}\binom{d}{g}\binom{d+g}{g}\binom{g}{z}(-1)^{g-z}2^{(b-1)z}\right.$$
$$\left.\times\frac{\Gamma(z+1)e^{-\frac{2c-2}{2^b}s}}{s^{z+1}} - \sum_{g=0}^{d}\binom{d}{g}\binom{d+g}{g}2^{(b-1)g}\frac{\Gamma(g+1)e^{-\frac{2c}{2^b}s}}{s^{g+1}}\right] \tag{2.53}$$

$$= \frac{1}{s^{\alpha}}\sqrt{\frac{2d+1}{2}}2^{b/2}\left[\sum_{g=0}^{d}\sum_{z=0}^{g}\binom{d}{g}\binom{d+g}{g}\binom{g}{z}(-1)^{g-z}2^{(b-1)z}\right.$$
$$\left.\times\Gamma(z+1)\frac{e^{-\frac{2c-2}{2^b}s}}{s^{z+1}} - \sum_{g=0}^{d}\binom{d}{g}\binom{d+g}{g}2^{(b-1)g}\Gamma(g+1)\frac{e^{-\frac{2c}{2^b}s}}{s^{g+1}}\right] \tag{2.54}$$

$$= \sqrt{\frac{2d+1}{2}} 2^{b/2} \left[\sum_{g=0}^{d} \sum_{z=0}^{g} \binom{d}{g} \binom{d+g}{g} \binom{g}{z} (-1)^{g-z} 2^{(b-1)z} \right.$$
$$\left. \times \Gamma(z+1) \frac{e^{-\frac{2c-2}{2^b}s}}{s^{\alpha+z+1}} - \sum_{g=0}^{d} \binom{d}{g} \binom{d+g}{g} 2^{(b-1)g} \Gamma(g+1) \frac{e^{-\frac{2c}{2^b}s}}{s^{\alpha+g+1}} \right]. \tag{2.55}$$

If the inverse Laplace transform is applied to both sides, we acquire ${}_0\mathcal{I}_t^{\alpha}\psi_{c,d}(t)$,

$${}_0\mathcal{I}_t^{\alpha}\psi_{c,d}(t) = \sqrt{\frac{2d+1}{2}} 2^{b/2} \left[\sum_{g=0}^{d} \sum_{z=0}^{g} \binom{d}{g} \binom{d+g}{g} \binom{g}{z} (-1)^{g-z} 2^{(b-1)z} \Gamma(z+1) \right.$$
$$\left. \times \mathcal{L}^{-1} \left\{ \frac{e^{-\frac{2c-2}{2^b}s}}{s^{\alpha+z+1}} \right\} - \sum_{g=0}^{d} \binom{d}{g} \binom{d+g}{g} 2^{(b-1)g} \Gamma(g+1) \mathcal{L}^{-1} \left\{ \frac{e^{-\frac{2c}{2^b}s}}{s^{\alpha+g+1}} \right\} \right]$$

(2.56)

$$= \sqrt{\frac{2d+1}{2}} 2^{b/2} \left[\sum_{g=0}^{d} \sum_{z=0}^{g} \binom{d}{g} \binom{d+g}{g} \binom{g}{z} (-1)^{g-z} 2^{(b-1)z} \Gamma(z+1) \right.$$
$$\times \frac{v_{\frac{2c-2}{2^b}}(t) \left(t - \frac{2c-2}{2^b} \right)^{\alpha+z}}{\Gamma(\alpha+z+1)} - \sum_{g=0}^{d} \binom{d}{g} \binom{d+g}{g} 2^{(b-1)g} \Gamma(g+1)$$
$$\left. \times \frac{v_{\frac{2c}{2^b}}(t) \left(t - \frac{2c}{2^b} \right)^{\alpha+g}}{\Gamma(\alpha+g+1)} \right]. \tag{2.57}$$

We can rewrite the Riemann-Liouville integral of order α of $\psi_{c,d}$ as a piecewise function.

$$
{}_0\mathcal{I}_t^{\alpha}\psi_{c,d}(t) = \begin{cases} 0, & \text{if} \quad t < \dfrac{2c-2}{2^b}; \\ \\ \sqrt{\dfrac{2d+1}{2}}2^{b/2} \\ \times \left[\displaystyle\sum_{g=0}^{d}\sum_{z=0}^{g} \binom{d}{g}\binom{d+g}{g}\binom{g}{z} \right. \\ \times (-1)^{g-z}2^{(b-1)z}\,\Gamma(z+1) \\ \left. \times \dfrac{\left(t-\dfrac{2c-2}{2^b}\right)^{\alpha+z}}{\Gamma(\alpha+z+1)} \right], & \text{if} \quad \dfrac{2c-2}{2^b} \le t < \dfrac{2c}{2^b}; \\ \\ \sqrt{\dfrac{2d+1}{2}}2^{b/2} \\ \times \left[\displaystyle\sum_{g=0}^{d}\sum_{z=0}^{g} \binom{d}{g}\binom{d+g}{g}\binom{g}{z} \right. \\ \times (-1)^{g-z}2^{(b-1)z}\,\Gamma(z+1) \\ \times \dfrac{\left(t-\dfrac{2c-2}{2^b}\right)^{\alpha+z}}{\Gamma(\alpha+z+1)} - \displaystyle\sum_{g=0}^{d} \binom{d}{g}\binom{d+g}{g} \\ \left. \times 2^{(b-1)g}\,\Gamma(g+1)\dfrac{\left(t-\dfrac{2c}{2^b}\right)^{\alpha+g}}{\Gamma(\alpha+g+1)} \right], & \text{if} \quad \dfrac{2c}{2^b} \le t. \end{cases} \tag{2.58}
$$

The proof is now complete. ■

CHAPTER 3

FRACTIONAL LANE-EMDEN TYPE EQUATIONS

For fractional Lane-Emden type equations, we will first introduce the quasilinearization technique. Then we will explain the proposed method. Convergence analysis will also be given. Finally, we will solve some numerical examples.

3.1 Quasilinearization

Fractional Lane-Emden type equations (1.3) are nonlinear equations. To make calculations easier, we should linearize them. For linearization, we use the quasilinearization technique, which was proposed by Bellman and Kalaba [4]. First, we need to rewrite fractional Lane-Emden type equations (1.3) in the following form

$$L\left(r, y, D^{\beta}y, D^{\alpha}y\right) + N\left(r, y, D^{\beta}, D^{\alpha}y\right) = 0, \tag{3.1}$$

where $D^{\beta}y$ and $D^{\alpha}y$ denote the Caputo fractional derivatives $\dfrac{d^{\beta}y(r)}{dr^{\beta}}$ and $\dfrac{d^{\alpha}y(r)}{dr^{\alpha}}$, respectively. $L\left(r, y, D^{\beta}y, D^{\alpha}y\right)$ is the linear part and $N\left(r, y, D^{\beta}y, D^{\alpha}y\right)$ is the nonlinear part of the equation. For fractional Lane-Emden type equations (1.3), the linear part is

$$L\left(r, y, D^{\beta}y, D^{\alpha}y\right) = \frac{d^{\alpha}y(r)}{dr^{\alpha}} + \frac{K}{r^{\alpha-\beta}}\frac{d^{\beta}y(r)}{dr^{\beta}}, \tag{3.2}$$

and the nonlinear part is

$$N\left(r, y, D^{\beta}y, D^{\alpha}y\right) = h(r, y(r)). \tag{3.3}$$

Suppose that we have an initial guess y_0 for the solution of fractional Lane-Emden

type equations (3.1). Then we can expand the nonlinear part N using the linear terms of the Taylor series around the initial guess y_0 as follows:

$$\begin{aligned} N\left(r, y, D^{\beta}y, D^{\alpha}y\right) \approx N\left(r, y_0, D^{\beta}y_0, D^{\alpha}y_0\right) &+ \frac{\partial}{\partial y}N\left(r, y_0, D^{\beta}y_0, D^{\alpha}y_0\right)(y - y_0) \\ &+ \frac{\partial}{\partial\, D^{\beta}y}N\left(r, y_0, D^{\beta}y_0, D^{\alpha}y_0\right)\left(D^{\beta}y - D^{\beta}y_0\right) \\ &+ \frac{\partial}{\partial\, D^{\alpha}y}N\left(r, y_0, D^{\beta}y_0, D^{\alpha}y_0\right)\left(D^{\alpha}y - D^{\alpha}y_0\right). \end{aligned} \tag{3.4}$$

The notation $\dfrac{\partial}{\partial\, D^{\beta}y}N\left(r, y_0, D^{\beta}y_0, D^{\alpha}y_0\right)$ indicates taking the partial derivative of the nonlinear part N with respect to $D^{\beta}y$ and evaluating the result for $\left(r, y_0, D^{\beta}y_0, D^{\alpha}y_0\right)$. Also, the notation $\dfrac{\partial}{\partial\, D^{\alpha}y}N\left(r, y_0, D^{\beta}y_0, D^{\alpha}y_0\right)$ indicates taking the partial derivative of the nonlinear part N with respect to $D^{\alpha}y$ and evaluating the result for $\left(r, y_0, D^{\beta}y_0, D^{\alpha}y_0\right)$. Note that the right hand side of approximation (3.4) is linear. Now, we can replace the nonlinear part of fractional Lane-Emden type equation (3.1) by the right-hand side of approximation (3.4). Then we can solve the resulting linear equation for y and call the solution y_1. Now, we can expand the nonlinear part N using the linear terms of the Taylor series around the approximate solution y_1. Using this approximation, we can solve the resulting linear equation for y and call it y_2. Continuing this way, the general method for the $(p+1)$-th iteration can be expressed as follows

$$\begin{aligned} N\left(r, y, D^{\beta}y, D^{\alpha}y\right) \approx N\left(r, y_p, D^{\beta}y_p, D^{\alpha}y_p\right) &+ \frac{\partial}{\partial y}N\left(r, y_p, D^{\beta}y_p, D^{\alpha}y_p\right)(y_{p+1} - y_p) \\ &+ \frac{\partial}{\partial\, D^{\beta}y}N\left(r, y_p, D^{\beta}y_p, D^{\alpha}y_p\right)\left(D^{\beta}y_{p+1} - D^{\beta}y_p\right) \\ &+ \frac{\partial}{\partial\, D^{\alpha}y}N\left(r, y_p, D^{\beta}y_p, D^{\alpha}y_p\right)\left(D^{\alpha}y_{p+1} - D^{\alpha}y_p\right). \end{aligned} \tag{3.5}$$

Since $N\left(r, y, D^{\beta}y, D^{\alpha}y\right) = h\left(r, y(r)\right)$ for fractional Lane-Emden type equation (3.1), we have

$$h\left(r, y(r)\right) \approx h(r, y_p(r)) + \frac{\partial}{\partial y} h(r, y_p(r)) \left(y_{p+1}(r) - y_p(r)\right). \tag{3.6}$$

So, in each iteration, we need to solve the equation for $y_{p+1}(t)$

$$\frac{d^\alpha y_{p+1}(r)}{dr^\alpha} + \frac{K}{r^{\alpha-\beta}} \frac{d^\beta y_{p+1}(r)}{dr^\beta} + h(r, y_p(r)) + \frac{\partial}{\partial y} h(r, y_p(r)) \left(y_{p+1}(r) - y_p(r)\right) = 0, \tag{3.7}$$

with the initial conditions

$$y_{p+1}(0) = P, \qquad y'_{p+1}(0) = Q. \tag{3.8}$$

Furthermore, Bellman and Kalaba [4] showed that the sequence $\{y_{p+1}\}_{p=0}^{\infty}$ converges quadratically to y if the sequence converges. Just like in the Newton-Raphson method for approximating roots of algebraic equations, the initial guess has a very crucial impact on the convergence of quasilinearization technique [24].

3.2 Description of the Proposed Method

Let $y_{p+1}(r)$ be the approximate solution of the nonlinear fractional Lane-Emden type equation (1.3) obtained by quasilinearization technique in the $(p+1)$-th iteration. Using Legendre wavelets, we can approximate $\dfrac{d^\alpha y_{p+1}(r)}{dr^\alpha}$ by

$$\frac{d^\alpha y_{p+1}(r)}{dr^\alpha} \approx \sum_{c=1}^{2^{b-1}} \sum_{d=0}^{D-1} a_{c,d}^{p+1} \psi_{c,d}(r). \tag{3.9}$$

By integrating both sides of equation (3.9) and using the initial conditions, we can approximate $\dfrac{d^\beta y_{p+1}(r)}{dr^\beta}$ and $y_{p+1}(r)$ as follows:

$$\frac{d^\beta y_{p+1}(r)}{dr^\beta} \approx \sum_{c=1}^{2^{b-1}} \sum_{d=0}^{D-1} a_{c,d}^{p+1} \left[{}_0\mathcal{I}_r^{\alpha-\beta} \psi_{c,d}(r)\right] + Q \frac{r^{1-\beta}}{\Gamma(2-\beta)}, \tag{3.10}$$

$$y_{p+1}(r) \approx \sum_{c=1}^{2^{b-1}} \sum_{d=0}^{D-1} a_{c,d}^{p+1} \left[{}_0\mathcal{I}_r^{\alpha} \psi_{c,d}(r) \right] + Qr + P. \tag{3.11}$$

If we replace $\approx$ by $=$ and put equation (3.9), equation (3.10), and equation (3.11), in equation (3.7), we get

$$\begin{aligned} &\sum_{c=1}^{2^{b-1}} \sum_{d=0}^{D-1} a_{c,d}^{p+1} \psi_{c,d}(r) + \frac{K}{r^{\alpha-\beta}} \left(\sum_{c=1}^{2^{b-1}} \sum_{d=0}^{D-1} a_{c,d}^{p+1} \left[{}_0\mathcal{I}_r^{\alpha-\beta} \psi_{c,d}(r) \right] + Q \frac{r^{1-\beta}}{\Gamma(2-\beta)} \right) \\ &+ h\left(r, y_p(r)\right) + \frac{\partial}{\partial y} h(r, y_p(r)) \left(\left(\sum_{c=1}^{2^{b-1}} \sum_{d=0}^{D-1} a_{c,d}^{p+1} \left[{}_0\mathcal{I}_r^{\alpha} \psi_{c,d}(r) \right] + Qr + P \right) - y_p(r) \right) \\ &= 0. \end{aligned} \tag{3.12}$$

If we solve the linear equation (3.12) at the collocation points $r_j = \dfrac{2j-1}{2^b D}$, where $j = 1, \ldots, 2^{b-1} D$, we can obtain the unknown coefficients $a_{c,d}^{p+1}$. We can find an approximate solution by substituting the coefficients $a_{c,d}^{p+1}$ into equation (3.11).

3.3 Convergence Analysis

Theorem 2. [44] Suppose that $y(r) \in L^2([0,1))$ is a real valued function with $|y''(r)| \leq C$, where $C \in \mathbb{R}^+$. Let $y_{b,D}(r)$ be the approximation in (2.20). Then we have

$$\|y(r) - y_{b,D}(r)\|_2^2 \leq \frac{3DC^2}{(2^{4b-1})\,(16D^4 - 40D^2 + 9)}. \tag{3.13}$$

Proof. Please see [44]. ■

From the above error estimation, it can be concluded that the approximation $y_{b,D}(r)$ converges to $y(r)$ in $L^2([0,1))$ as b or D goes to infinity.

3.4 Numerical Examples

We will solve some examples to illustrate the effectiveness of the Legendre wavelet collocation method with quasilinearization technique (LWCMQT). In addition, maximum absolute errors

$$E_{L_\infty} := \max \left| y_{exact}(r_j) - y_{approximate}(r_j) \right|, \tag{3.14}$$

where the maximum is taken over all collocation points r_j, will be compared with some other methods in the literature. All calculations and graphs were obtained using Wolfram Mathematica Online [16].

Example 3.1. In the first example, we consider

$$\frac{d^\alpha y(r)}{dr^\alpha} + \frac{2}{r^{\alpha-\beta}} \frac{d^\beta y(r)}{dr^\beta} + y^m(r) = 0, \tag{3.15}$$

with

$$y(0) = 1, \qquad y'(0) = 0. \tag{3.16}$$

When $\alpha = 2$ and $\beta = 1$, the exact solutions are known only for $m = 0, 1, 5$ [6]. In this example, we will solve equation (3.15) for $m = 1$ and $m = 5$.

- Example 3.1.a: When $m = 1$, equation (3.15) becomes

$$\frac{d^\alpha y(r)}{dr^\alpha} + \frac{2}{r^{\alpha-\beta}} \frac{d^\beta y(r)}{dr^\beta} + y(r) = 0, \tag{3.17}$$

with

$$y(0) = 1, \qquad y'(0) = 0, \tag{3.18}$$

which is a linear equation. Hence, we do not need to apply the quasilinearization technique. If we take $\alpha = 2$ and $\beta = 1$, equation (3.17) with initial conditions (3.18) has the exact solution

$$y_{exact}(r) = \frac{\sin(r)}{r}. \tag{3.19}$$

We solve equation (3.17) using Legendre wavelet method. In Table 3.1, we compare maximum absolute errors of Haar Wavelet Collocation Method (HWCM) [34], Haar Wavelet Collocation Adomian Method (HWCAM) [32], Chebyshev Wavelet Collocation Quasilinearization Method (CWCQM) [27], and Legendre Wavelet Collocation Method with Quasilinearization Technique (LWCMQT) for $\alpha = 2$ and $\beta = 1$. Figure 3.1 shows the graphs of numerical solutions for various pairs of α and β. The graphs of approximate solution and exact solution for $\alpha = 2$, $\beta = 1$ and $b = 2$, $D = 8$ are plotted in Figure 3.2. Moreover, we plot the absolute error for $\alpha = 2$, $\beta = 1$ and $b = 2$, $D = 8$ in Figure 3.3.

Table 3.1. Maximum absolute errors (E_{L_∞}) for $\alpha = 2$ and $\beta = 1$ obtained by various numerical methods in Example 3.1.a

Number of Col. Pts.	HWCM E_{L_∞}	HWCAM E_{L_∞}	CWCQM E_{L_∞}	LWCMQT E_{L_∞}
8	$1.8562E-05$	$7.2156E-05$	$6.7870E-08$	$2.5801E-13$
16	$5.0012E-06$	$4.3274E-05$	$1.1146E-11$	$1.6098E-14$
32	$1.2932E-06$	$1.0015E-05$	$9.6485E-12$	$2.2204E-16$

- Example 3.1.b: When $m = 5$, equation (3.15) becomes

$$\frac{d^\alpha y(r)}{dr^\alpha} + \frac{2}{r^{\alpha-\beta}}\frac{d^\beta y(r)}{dr^\beta} + y^5(r) = 0, \tag{3.20}$$

with

Figure 3.1. The graphs of numerical solutions for various pairs of α and β in Example 3.1.a obtained by LWCMQT with $b = 3$ and $D = 8$.

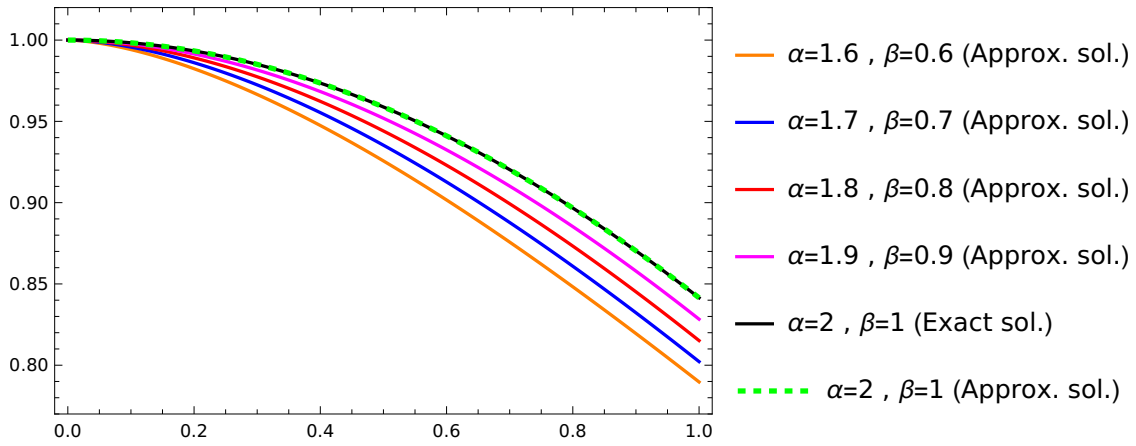

Figure 3.2. Exact solution and approximate solution of Example 3.1.a for $\alpha = 2$, $\beta = 1$ and $b = 2$, $D = 8$ obtained by LWCMQT.

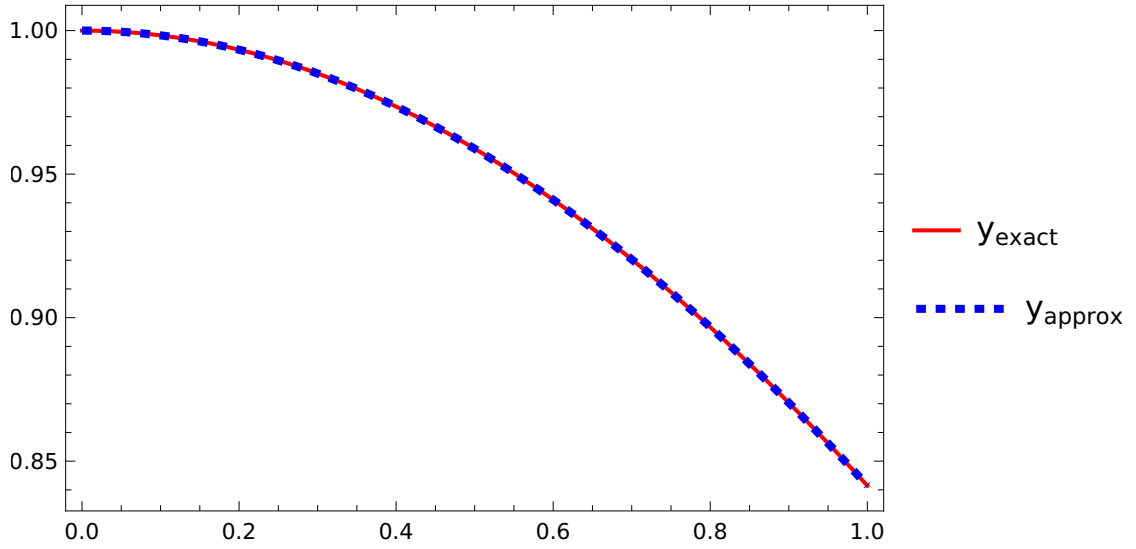

$$y(0) = 1, \qquad y'(0) = 0. \tag{3.21}$$

If we take $\alpha = 2$ and $\beta = 1$, equation (3.20) with initial conditions (3.21) has the exact solution

$$y_{exact}(r) = \frac{1}{\sqrt{1 + \frac{r^2}{3}}}. \tag{3.22}$$

Figure 3.3. Absolute error $|y_{exact}(r) - y_{approximate}(r)|$ in Example 3.1.a for $\alpha = 2$, $\beta = 1$ and $b = 2$, $D = 8$.

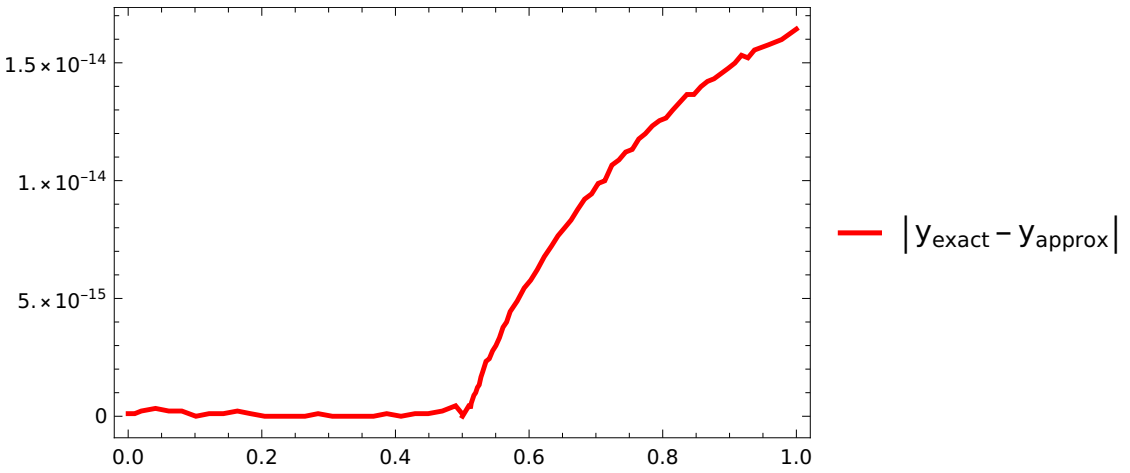

We use $y_0(r) = 1$ as an initial guess and implement the Legendre wavelet collocation method with quasilinearization technique. We iterate the quasilinearization technique three times. In Table 3.2, we compare maximum absolute errors of Haar Wavelet Collocation Method (HWCM) [34], Haar Wavelet Collocation Adomian Method (HWCAM) [32], Chebyshev Wavelet Collocation Quasilinearization Method (CWCQM) [27], and Legendre Wavelet Collocation Method with Quasilinearization Technique (LWCMQT) for $\alpha = 2$ and $\beta = 1$. Approximate solutions for various pairs of α and β are plotted in Figure 3.4. For $\alpha = 2$, $\beta = 1$ and $b = 3$, $D = 8$, the plot of the exact solution along with the plots of numerical solutions in the first, second, and third iteration are drawn in Figure 3.5. Moreover, we plot the absolute errors in the first, second, and third iteration for $\alpha = 2$, $\beta = 1$ and $b = 3$, $D = 8$ in Figure 3.6.

Table 3.2. Maximum absolute errors (E_{L_∞}) for $\alpha = 2$ and $\beta = 1$ obtained by various numerical methods in Example 3.1.b

Number of Col. Pts.	HWCM E_{L_∞}	HWCAM E_{L_∞}	CWCQM E_{L_∞}	LWCMQT E_{L_∞}
8	$9.2374E-05$	$7.7048E-05$	$4.0104E-07$	$6.1911E-09$
16	$2.4231E-05$	$1.0573E-05$	$7.7340E-11$	$8.4153E-11$
32	$6.2101E-06$	$4.3726E-06$	$1.8416E-11$	$6.7579E-13$

Figure 3.4. The graphs of numerical solutions for various pairs of α and β in Example 3.1.b obtained by LWCMQT with $b = 3$ and $D = 8$ in the third iteration.

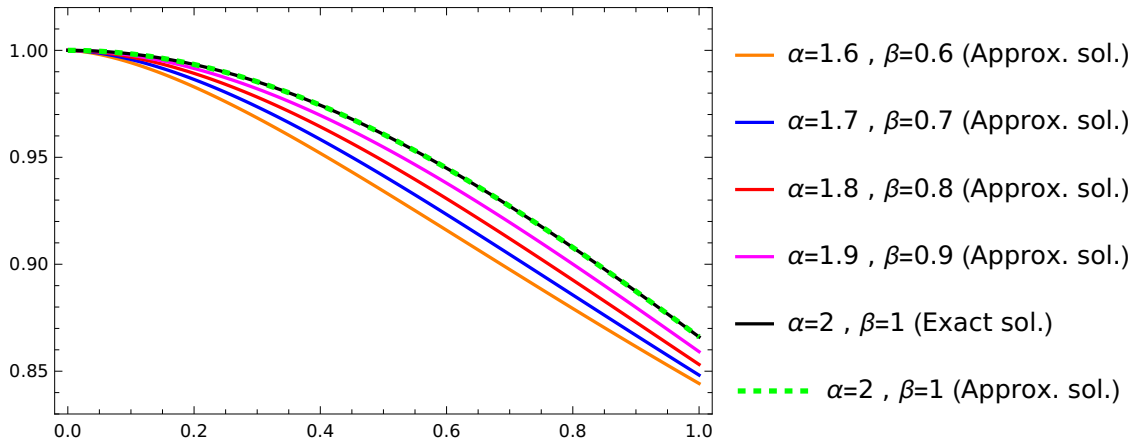

Example 3.2. In the second example, we consider

$$\frac{d^{\alpha}y(r)}{dr^{\alpha}} + \frac{2}{r^{\alpha-\beta}}\frac{d^{\beta}y(r)}{dr^{\beta}} + 8e^{y(r)} + 4e^{\frac{y(r)}{2}} = 0, \tag{3.23}$$

with

$$y(0) = 0, \qquad y'(0) = 0. \tag{3.24}$$

If we take $\alpha = 2$ and $\beta = 1$, the function

$$y_{exact}(r) = -2\ln(1 + r^2). \tag{3.25}$$

is the exact solution of equation (3.23) with initial conditions (3.24). We use $y_0(r) = 0$ as an initial guess and implement the Legendre wavelet collocation method with quasilinearization technique. We iterate the quasilinearization technique three times. For $\alpha = 2$, $\beta = 1$ and $b = 2$, $D = 8$, we present the numerical results obtained by Adomian Decomposition Method (ADM) [42], Haar Wavelet Collocation Method (HWCM) [34], Chebyshev Wavelet Collocation Quasilinearization Method (CWCQM) [27], and Legendre Wavelet

Figure 3.5. For $\alpha = 2$ and $\beta = 1$, the plot of the exact solution along with the plots of numerical solutions in the first, second, and third iteration in Example 3.1.b obtained by LWCMQT with $b = 3$ and $D = 8$

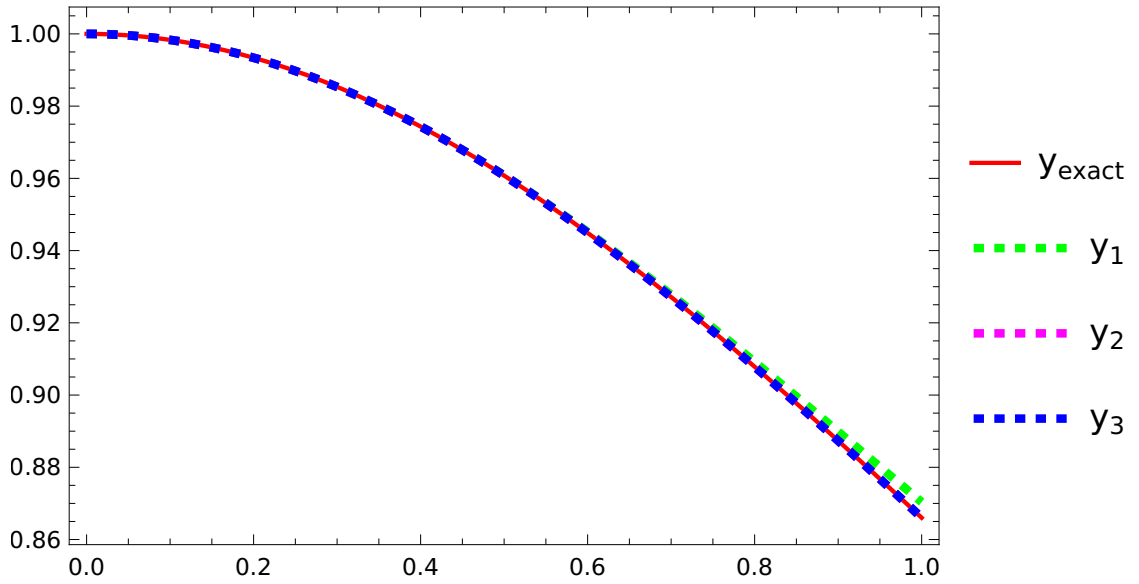

Collocation Method with Quasilinearization Technique(LWCMQT) in the third iteration in Table 3.3. Approximate solutions for various pairs of α and β are plotted in Figure 3.7. For $\alpha = 2$, $\beta = 1$ and $b = 3$, $D = 8$, the plot of the exact solution along with the plots of numerical solutions in the first, second, and third iteration are drawn in Figure 3.8. Moreover, for $\alpha = 2$, $\beta = 1$, we plot the absolute errors in the first, second, and third iteration for $b = 3$, $D = 8$ in Figure 3.9.

Example 3.3. In the last example, we consider

$$\frac{d^{\alpha}y(r)}{dr^{\alpha}} + \frac{2}{r^{\alpha-\beta}}\frac{d^{\beta}y(r)}{dr^{\beta}} + e^{y(r)}\left(6 - 4r^2e^{y(r)}\right) = 0, \tag{3.26}$$

with

$$y(0) = -\ln(4), \qquad y'(0) = 0. \tag{3.27}$$

If we take $\alpha = 2$ and $\beta = 1$, equation (3.26) with initial conditions (3.27) has the exact solution

$$y_{exact}(r) = \ln\left(\frac{1}{r^2+4}\right). \tag{3.28}$$

We use $y_0(r) = -\ln(4)$ as an initial guess and implement the Legendre wavelet collocation method with quasilinearization technique. We iterate the quasilinearization technique three times. In Table 3.4, we compare maximum absolute errors of Haar Wavelet Collocation Method (HWCM) [34], Chebyshev Wavelet Collocation Quasilinearization Method (CWCQM) [27], and Legendre Wavelet Collocation Method with Quasilinearization Technique(LWCMQT) for $\alpha = 2$ and $\beta = 1$. Approximate solutions for various pairs of α and β are plotted in Figure 3.10. For $\alpha = 2$, $\beta = 1$ and $b = 3$, $D = 8$, the plot of the exact solution along with the plots of numerical solutions in the first, second, and third iteration are drawn in Figure 3.11. Moreover, we plot the absolute errors in the first, second, and third iteration for $\alpha = 2$, $\beta = 1$ and $b = 3$, $D = 8$ in Figure 3.12.

Figure 3.6. For $\alpha = 2$, $\beta = 1$, and $b = 3$, $D = 8$, the graphs of absolute errors in Example 3.1.b

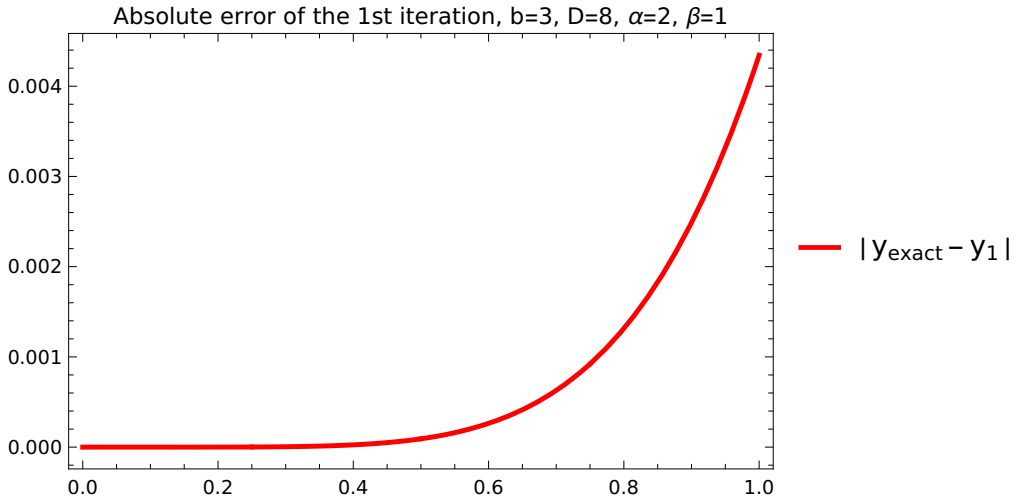

(a) Absolute error of the first iteration $|y_{exact}(r) - y_1(r)|$ in Example 3.1.b

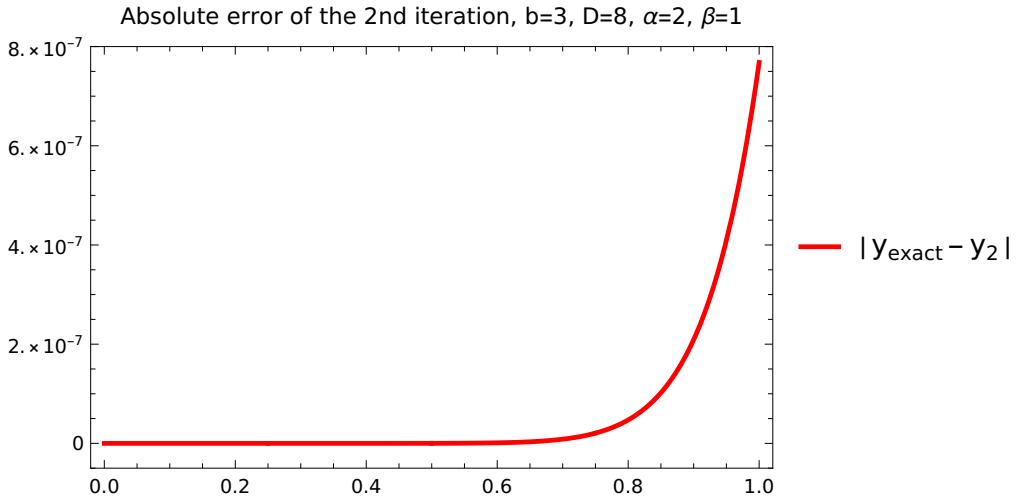

(b) Absolute error of the second iteration $|y_{exact}(r) - y_2(r)|$ in Example 3.1.b

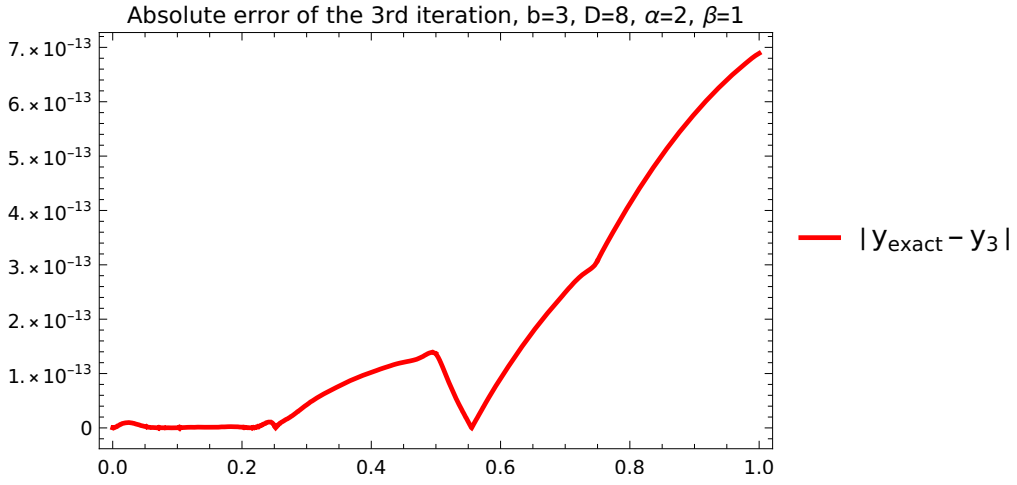

(c) Absolute error of the third iteration $|y_{exact}(r) - y_3(r)|$ in Example 3.1.b

Table 3.3. Numerical results for $\alpha = 2$, $\beta = 1$ and $b = 2$, $D = 8$ in Example 3.2 obtained by ADM, HWCM, CWCQM, and LWCMQT in the third iteration.

Col. Pts. r	Exact Sol. $y_{exact}(r)$	ADM $y_{ADM}(r)$	HWCM $y_{HWCM}(r)$	CWCQM $y_{CWCQM}(r)$	LWCMQT $y_{LWCMQT}(r)$
$\frac{1}{32}$	-0.001952	-0.001952	-0.001949	-0.001952	-0.001952
$\frac{3}{32}$	-0.017501	-0.017501	-0.017504	-0.017501	-0.017501
$\frac{5}{32}$	-0.048241	-0.048241	-0.048255	-0.048241	-0.048241
$\frac{7}{32}$	-0.093483	-0.093483	-0.093513	-0.093483	-0.093483
$\frac{9}{32}$	-0.152257	-0.152257	-0.152309	-0.152257	-0.152257
$\frac{11}{32}$	-0.223376	-0.223376	-0.223454	-0.223376	-0.223376
$\frac{13}{32}$	-0.305509	-0.305508	-0.305619	-0.305509	-0.305509
$\frac{15}{32}$	-0.397253	-0.397247	-0.397399	-0.397253	-0.397253
$\frac{17}{32}$	-0.497196	-0.497163	-0.497381	-0.497196	-0.497196
$\frac{19}{32}$	-0.603967	-0.603819	-0.604194	-0.603967	-0.603967
$\frac{21}{32}$	-0.716277	-0.715706	-0.716548	-0.716277	-0.716277
$\frac{23}{32}$	-0.832944	-0.831008	-0.833257	-0.832944	-0.832944
$\frac{25}{32}$	-0.952905	-0.947015	-0.953261	-0.952905	-0.952905
$\frac{27}{32}$	-1.075224	-1.058866	-1.075621	-1.075224	-1.075224
$\frac{29}{32}$	-1.199089	-1.157061	-1.199524	-1.199089	-1.199089
$\frac{31}{32}$	-1.323804	-1.222860	-1.324275	-1.323804	-1.323804

Figure 3.7. Numerical solutions for various pairs of α and β in Example 3.2 obtained by LWCMQT with $b = 3$ and $D = 8$ in the third iteration.

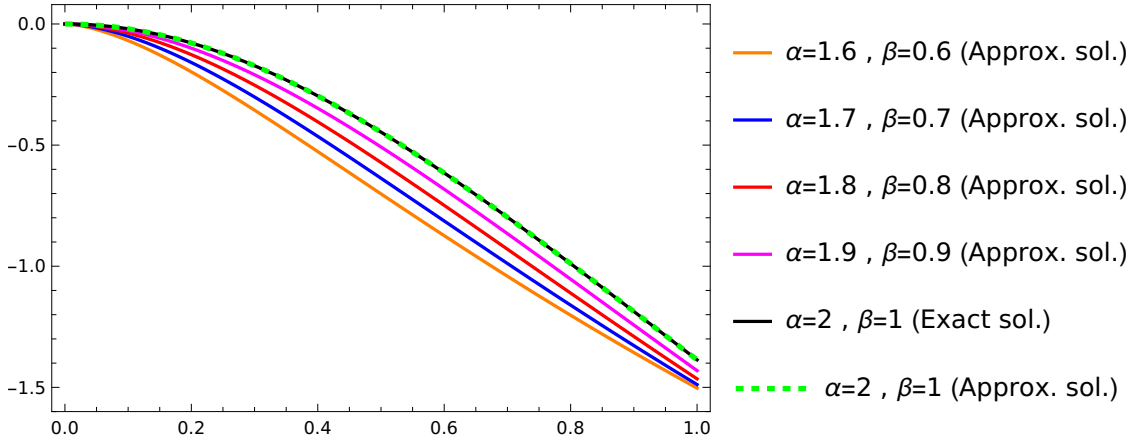

Figure 3.8. For $\alpha = 2$ and $\beta = 1$, the plot of the exact solution along with the plots of numerical solutions in the first, second, and third iteration in Example 3.2 obtained by LWCMQT with $b = 3$ and $D = 8$

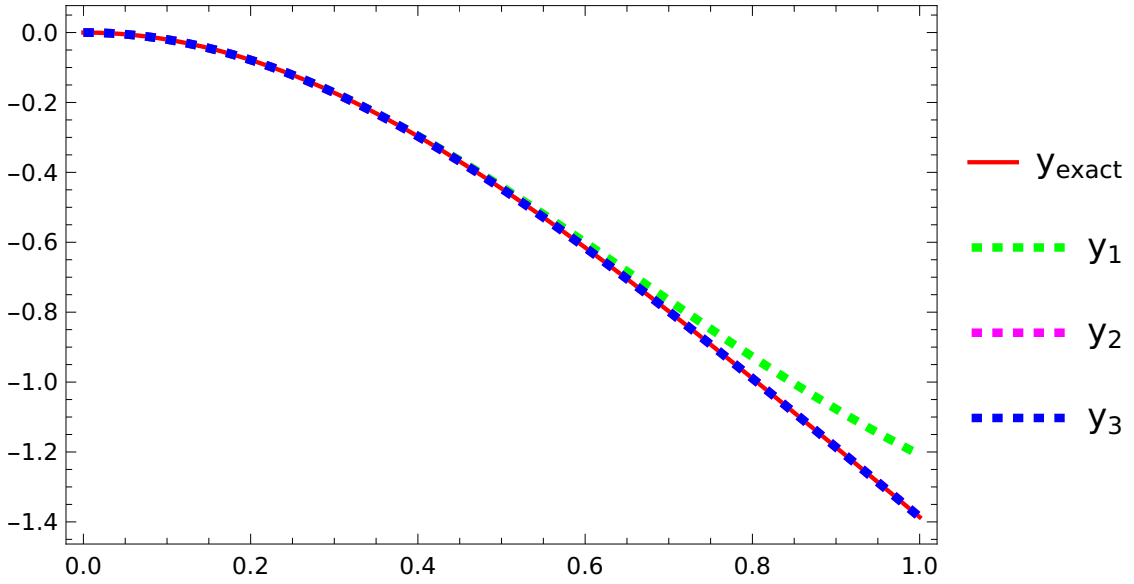

Table 3.4. Maximum absolute errors (E_{L_∞}) for $\alpha = 2$ and $\beta = 1$ obtained by various numerical methods in Example 3.3

Number of Col. Pts.	HWCM E_{L_∞}	CWCQM E_{L_∞}	LWCMQT E_{L_∞}
8	$8.94E-05$	$5.32E-07$	$1.16E-09$
16	$2.02E-05$	$3.70E-12$	$1.41E-11$
32	$5.22E-06$	$1.25E-14$	$1.32E-13$

Figure 3.9. For $\alpha = 2$, $\beta = 1$, and $b = 3$, $D = 8$, the graphs of absolute errors in Example 3.2

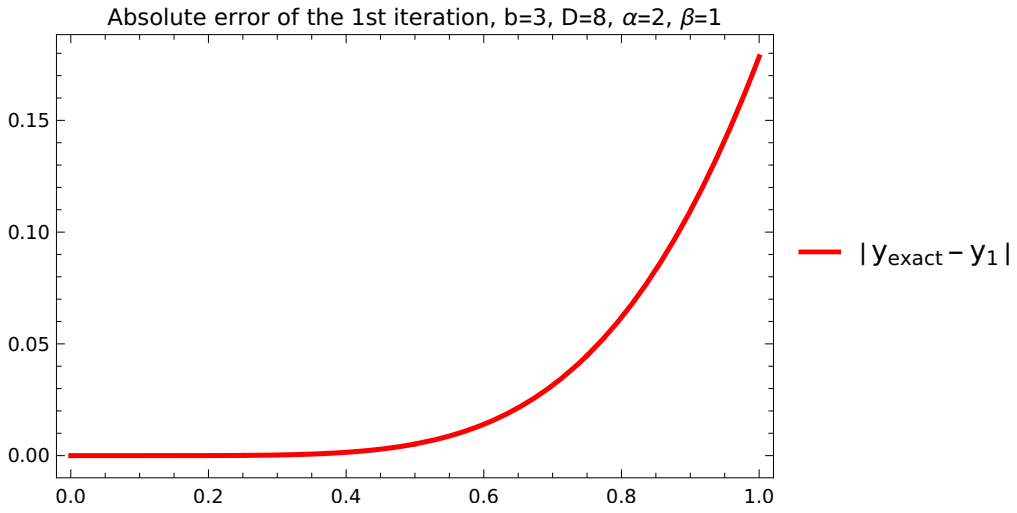

(a) Absolute error of the first iteration $|y_{exact}(r) - y_1(r)|$ in Example 3.2

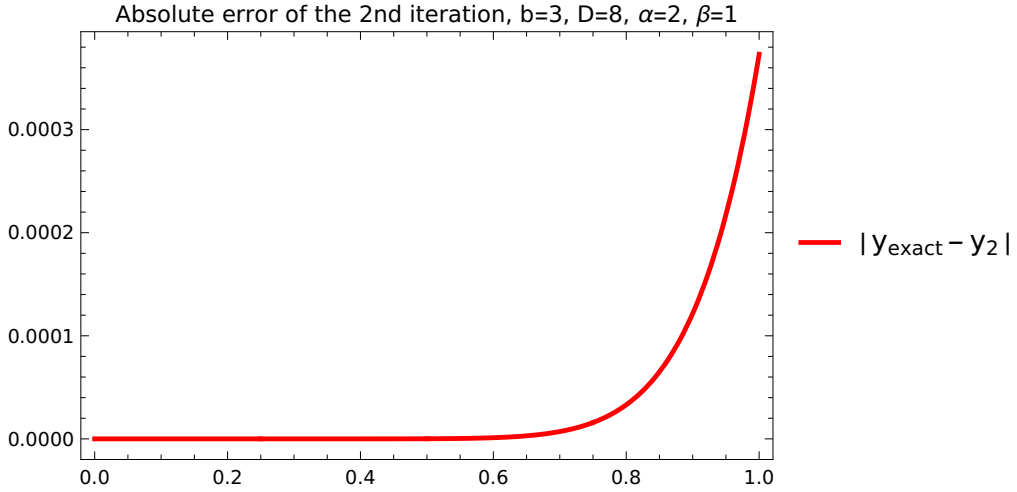

(b) Absolute error of the second iteration $|y_{exact}(r) - y_2(r)|$ in Example 3.2

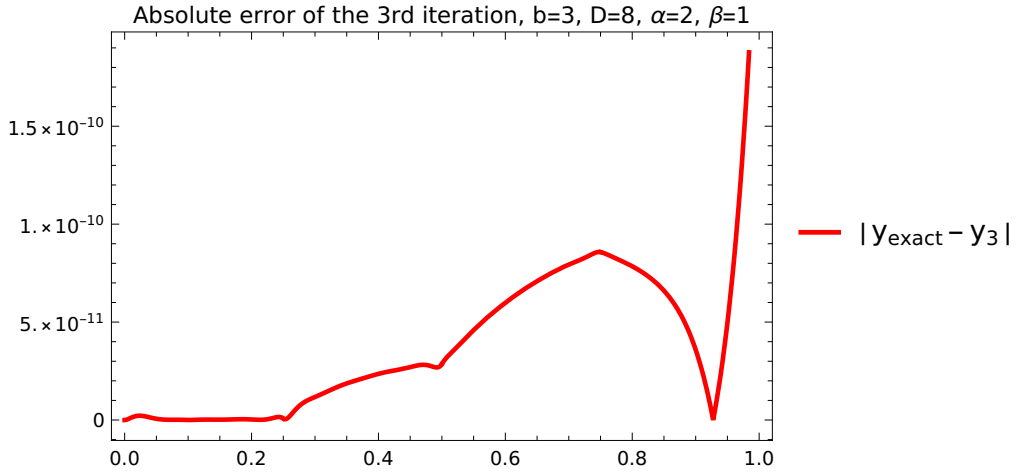

(c) Absolute error of the third iteration $|y_{exact}(r) - y_3(r)|$ in Example 3.2

Figure 3.10. Numerical solutions for various pairs of α and β in Example 3.3 obtained by LWCMQT with $b = 3$ and $D = 8$ in the third iteration.

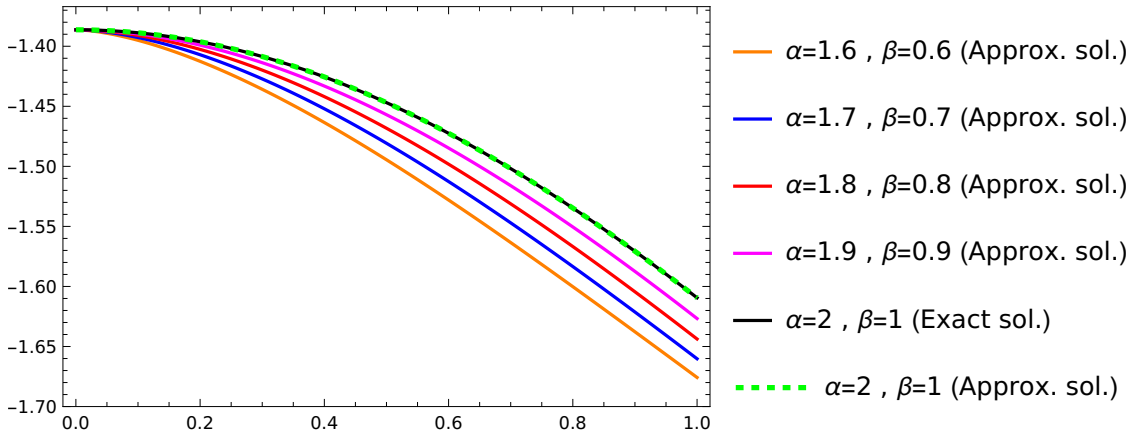

Figure 3.11. For $\alpha = 2$ and $\beta = 1$, the plot of the exact solution along with the plots of numerical solutions in the first, second, and third iteration in Example 3.3 obtained by LWCMQT with $b = 3$ and $D = 8$

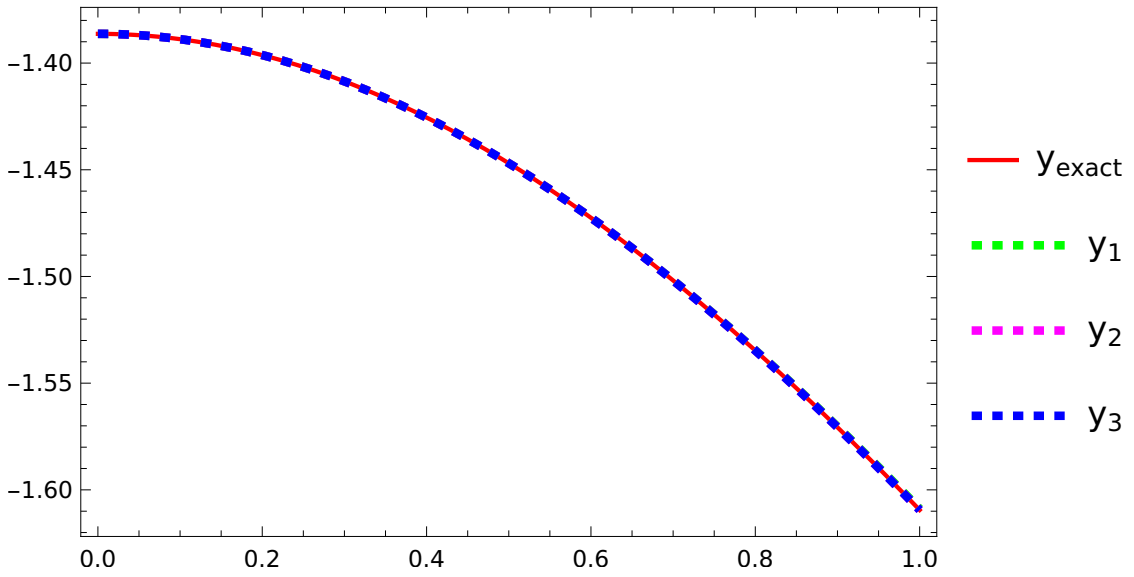

Figure 3.12. For $\alpha = 2$, $\beta = 1$, and $b = 3$, $D = 8$, the graphs of absolute errors in Example 3.3

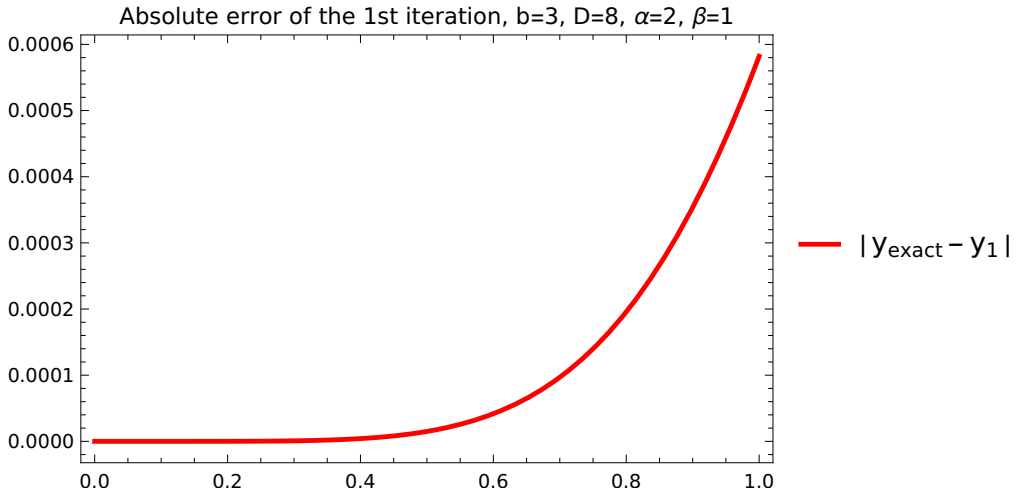

(a) Absolute error of the first iteration $|y_{exact}(r) - y_1(r)|$ in Example 3.3

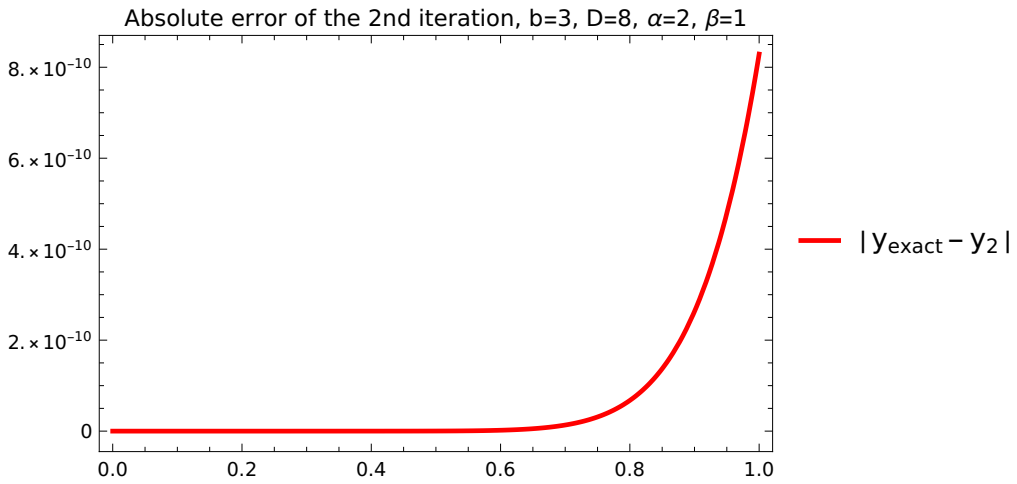

(b) Absolute error of the second iteration $|y_{exact}(r) - y_2(r)|$ in Example 3.3

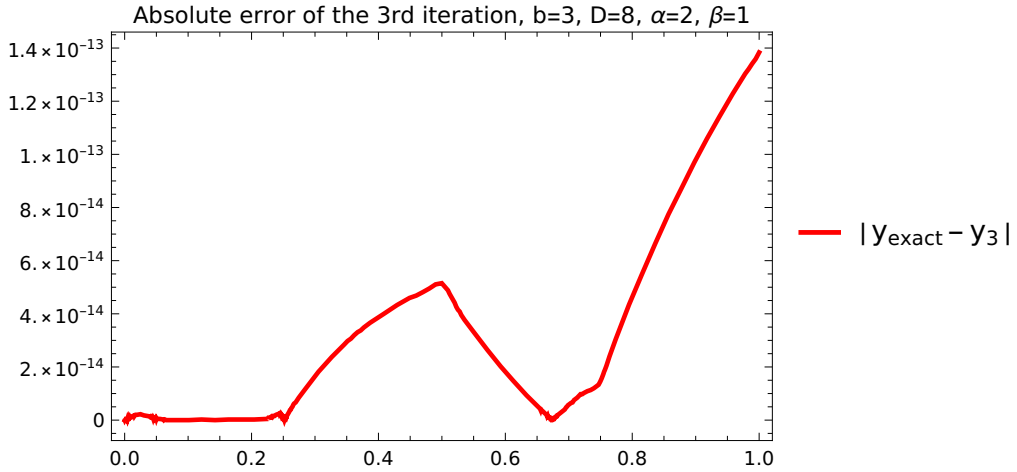

(c) Absolute error of the third iteration $|y_{exact}(r) - y_3(r)|$ in Example 3.3

CHAPTER 4

TIME-FRACTIONAL FISHER'S EQUATION

In this chapter, we will describe the quasilinearization technique for the time-fractional Fisher's equation. After that, we will explain the proposed method and study the convergence analysis. Lastly, we will solve some numerical examples.

4.1 Quasilinearization

The time-fractional Fisher's equation (1.5) is a nonlinear equation. For ease of computation, we should linearize it. For this purpose, we employ the quasilinearization technique, which was presented by Bellman and Kalaba [4]. First, we need to rewrite the modified time-fractional Fisher's equation (1.5) in the following form

$$L\left(y, Dy, D^2y\right) + N\left(y, Dy, D^2y\right) + q(x,t) = \frac{\partial^\alpha y(x,t)}{\partial t^\alpha}, \tag{4.1}$$

where Dy and D^2y denote the partial derivatives $\frac{\partial y}{\partial x}$ and $\frac{\partial^2 y}{\partial x^2}$, respectively. $L\left(y, Dy, D^2y\right)$ consists of linear terms and $N\left(y, Dy, D^2y\right)$ consists of nonlinear terms of the equation. For the time-fractional Fisher's equation (1.5), the linear part is

$$L\left(y, Dy, D^2y\right) = \delta\frac{\partial^2 y(x,t)}{\partial x^2} + \lambda y(x,t), \tag{4.2}$$

and the nonlinear part is

$$N\left(y, Dy, D^2y\right) = -\lambda y^{p+1}(x,t). \tag{4.3}$$

Suppose we have an initial guess y_0 for the solution of the time-fractional Fisher's equation (4.1). The nonlinear part N can be approximated by expanding the Taylor series around the initial guess y_0 and using only linear terms as follows:

$$\begin{aligned} N\left(y, Dy, D^2y\right) \approx N\left(y_0, Dy_0, D^2y_0\right) &+ \frac{\partial}{\partial y} N\left(y_0, Dy_0, D^2y_0\right)(y - y_0) \\ &+ \frac{\partial}{\partial\, Dy} N\left(y_0, Dy_0, D^2y_0\right)(Dy - Dy_0) \\ &+ \frac{\partial}{\partial\, D^2y} N\left(y_0, Dy_0, D^2y_0\right)(D^2y - D^2y_0). \end{aligned} \tag{4.4}$$

Here, $\dfrac{\partial}{\partial\, D^2y} N\left(y_0, Dy_0, D^2y_0\right)$ means that we first take the partial derivative of the nonlinear part N with respect to D^2y and then evaluate the result for (y_0, Dy_0, D^2y_0). Similarly, $\dfrac{\partial}{\partial\, Dy} N\left(y_0, Dy_0, D^2y_0\right)$ means that we first take the partial derivative of the nonlinear part N with respect to Dy and then evaluate the result for (y_0, Dy_0, D^2y_0). It should be noted that the right-hand side of approximation (4.4) is linear. Now, we can replace the nonlinear part of the time-fractional Fisher equation (4.1) by the right hand side of approximation (4.4). Then we can solve the resulting linear equation for y and call the solution y_1. Again, the nonlinear part N can be approximated by expanding the Taylor series around the approximate solution y_1 and using only linear terms. Using this approximation, we can solve the resulting linear equation for y and call it y_2. Continuing this way, the general method for the $(r+1)$-th iteration can be written as follows

$$\begin{aligned} N\left(y, Dy, D^2y\right) \approx N\left(y_r, Dy_r, D^2y_r\right) &+ \frac{\partial}{\partial y} N\left(y_r, Dy_r, D^2y_r\right)(y_{r+1} - y_r) \\ &+ \frac{\partial}{\partial\, Dy} N\left(y_r, Dy_r, D^2y_r\right)(Dy_{r+1} - Dy_r) \\ &+ \frac{\partial}{\partial\, D^2y} N\left(y_r, Dy_r, D^2y_r\right)(D^2y_{r+1} - D^2y_r). \end{aligned} \tag{4.5}$$

Since $N\left(y, Dy, D^2y\right) = -\lambda y^{p+1}$ for the time-fractional Fisher's equation (4.1), we have

$$-\lambda y^{p+1} \approx -\lambda y_r^{p+1} - \lambda\left((p+1)(y_r^p)\right)(y_{r+1} - y_r) \tag{4.6}$$

$$= -\lambda y_r^{p+1} - \lambda(p+1) y_r^p y_{r+1} + \lambda(p+1) y_r^{p+1}. \tag{4.7}$$

So, in each iteration, we need to solve the equation

$$\begin{aligned}&\delta\frac{\partial^2 y_{r+1}(x,t)}{\partial x^2}+\lambda y_{r+1}(x,t)+q(x,t)-\lambda(p+1)y_r^p(x,t)y_{r+1}(x,t)+\lambda p y_r^{p+1}(x,t)\\&=\frac{\partial^\alpha y_{r+1}(x,t)}{\partial t^\alpha},\end{aligned}\tag{4.8}$$

which can be rearranged as

$$\begin{aligned}&\delta\frac{\partial^2 y_{r+1}(x,t)}{\partial x^2}+\left(\lambda-\lambda(p+1)y_r^p(x,t)\right)y_{r+1}(x,t)+q(x,t)+\lambda p y_r^{p+1}(x,t)\\&=\frac{\partial^\alpha y_{r+1}(x,t)}{\partial t^\alpha},\end{aligned}\tag{4.9}$$

with the initial condition

$$y_{r+1}(x,0)=w(x),\tag{4.10}$$

and boundary conditions

$$y_{r+1}(0,t)=z_1(t),\tag{4.11}$$

$$y_{r+1}(1,t)=z_2(t).\tag{4.12}$$

Furthermore, Bellman and Kalaba [4] showed that the sequence $\{y_{r+1}\}_{r=0}^{\infty}$ converges quadratically to y if the sequence converges. Just like in the Newton-Raphson method for approximating roots of algebraic equations, the initial guess has a very crucial impact on the convergence of quasilinearization technique [24].

4.2 Description of the Proposed Method

Let $y_{r+1}(x,t)$ be the approximate solution of the nonlinear time-fractional Fisher's equation (1.5) obtained by quasilinearization technique in the $(r+1)$-th iteration. Using

Legendre wavelets, we can approximate $\dfrac{\partial^{2+\alpha} y_{r+1}(x,t)}{\partial x^2 \partial t^\alpha}$ by

$$\frac{\partial^{2+\alpha} y_{r+1}(x,t)}{\partial x^2 \partial t^\alpha} \approx \sum_{i=1}^{2^{b-1}D} \sum_{j=1}^{2^{h-1}Q} a_{i,j}^{r+1} \psi_i(x) \psi_j(t). \tag{4.13}$$

Taking the α-th order fractional integral of both sides of equation (4.13) with respect to t, we obtain

$$\frac{\partial^2 y_{r+1}(x,t)}{\partial x^2} \approx \left.\frac{\partial^2 y_{r+1}(x,t)}{\partial x^2}\right|_{t=0} + \sum_{i=1}^{2^{b-1}D} \sum_{j=1}^{2^{h-1}Q} a_{i,j}^{r+1} \psi_i(x) \left[{}_0\mathcal{I}_t^\alpha \psi_j(t)\right]. \tag{4.14}$$

Since $\left.\dfrac{\partial^2 y_{r+1}(x,t)}{\partial x^2}\right|_{t=0} = y''_{r+1}(x,0) = f''(x)$ by the initial condition, we can write

$$\frac{\partial^2 y_{r+1}(x,t)}{\partial x^2} \approx f''(x) + \sum_{i=1}^{2^{b-1}D} \sum_{j=1}^{2^{h-1}Q} a_{i,j}^{r+1} \psi_i(x) \left[{}_0\mathcal{I}_t^\alpha \psi_j(t)\right]. \tag{4.15}$$

Integrating equation (4.15) with respect to x from 0 to x, we get

$$\frac{\partial y_{r+1}(x,t)}{\partial x} \approx \left.\frac{\partial y_{r+1}(x,t)}{\partial x}\right|_{x=0} + f'(x) - f'(0) \tag{4.16}$$

$$+ \sum_{i=1}^{2^{b-1}D} \sum_{j=1}^{2^{h-1}Q} a_{i,j}^{r+1} \left[{}_0\mathcal{I}_x^1 \psi_i(x)\right] \left[{}_0\mathcal{I}_t^\alpha \psi_j(t)\right]. \tag{4.17}$$

Integrating equation (4.16) with respect to x from 0 to x, we get

$$\begin{aligned} y_{r+1}(x,t) \approx y_{r+1}(0,t) + x\left(\left.\frac{\partial y_{r+1}(x,t)}{\partial x}\right|_{x=0}\right) + w(x) - w(0) - xw'(0) \\ + \sum_{i=1}^{2^{b-1}D} \sum_{j=1}^{2^{h-1}Q} a_{i,j}^{r+1} \left[{}_0\mathcal{I}_x^2 \psi_i(x)\right] \left[{}_0\mathcal{I}_t^\alpha \psi_j(t)\right]. \end{aligned} \tag{4.18}$$

Now, let us evaluate equation (4.18) at $x = 1$.

$$\begin{aligned} y_{r+1}(1,t) \approx y_{r+1}(0,t) + 1\left(\left.\frac{\partial y_{r+1}(x,t)}{\partial x}\right|_{x=0}\right) + w(1) - w(0) - 1w'(0) \\ + \sum_{i=1}^{2^{b-1}D}\sum_{j=1}^{2^{h-1}Q} a_{i,j}^{r+1}\left[{}_0\mathcal{I}_x^2\psi_i(x)\right]_{x=1}\left[{}_0\mathcal{I}_t^\alpha\psi_j(t)\right]. \end{aligned} \tag{4.19}$$

Using the boundary conditions, we can write

$$\begin{aligned} z_2(t) \approx z_1(t) + \left(\left.\frac{\partial y_{r+1}(x,t)}{\partial x}\right|_{x=0}\right) + w(1) - w(0) - w'(0) \\ + \sum_{i=1}^{2^{b-1}D}\sum_{j=1}^{2^{h-1}Q} a_{i,j}^{r+1}\left[{}_0\mathcal{I}_x^2\psi_i(x)\right]_{x=1}\left[{}_0\mathcal{I}_t^\alpha\psi_j(t)\right]. \end{aligned} \tag{4.20}$$

Thus, we have

$$\begin{aligned} \left(\left.\frac{\partial y_{r+1}(x,t)}{\partial x}\right|_{x=0}\right) \approx z_2(t) - z_1(t) + w(0) + w'(0) - w(1) \\ - \sum_{i=1}^{2^{b-1}D}\sum_{j=1}^{2^{h-1}Q} a_{i,j}^{r+1}\left[{}_0\mathcal{I}_x^2\psi_i(x)\right]_{x=1}\left[{}_0\mathcal{I}_t^\alpha\psi_j(t)\right]. \end{aligned} \tag{4.21}$$

If we put equation (4.21) in equation (4.18), we get

$$\begin{aligned} y_{r+1}(x,t) \approx\ z_1(t) + x\Bigg(z_2(t) - z_1(t) + w(0) + w'(0) - w(1) \\ - \sum_{i=1}^{2^{b-1}D}\sum_{j=1}^{2^{h-1}Q} a_{i,j}\left[{}_0\mathcal{I}_x^2\psi_i(x)\right]_{x=1}\left[{}_0\mathcal{I}_t^\alpha\psi_j(t)\right]\Bigg) + w(x) - w(0) \\ - xw'(0) + \sum_{i=1}^{2^{b-1}D}\sum_{j=1}^{2^{h-1}Q} a_{i,j}^{r+1}\left[{}_0\mathcal{I}_x^2\psi_i(x)\right]\left[{}_0\mathcal{I}_t^\alpha\psi_j(t)\right]. \end{aligned} \tag{4.22}$$

Taking the α-th order Caputo derivative of both sides of equation (4.22) with respect to t yields

$$\begin{aligned}\frac{\partial^\alpha y_{r+1}(x,t)}{\partial t^\alpha} \approx \left[{}_0^C\mathcal{D}_t^\alpha z_1(t)\right] + x\Bigg(& \left[{}_0^C\mathcal{D}_t^\alpha z_2(t)\right] - \left[{}_0^C\mathcal{D}_t^\alpha z_1(t)\right] \\ & - \sum_{i=1}^{2^{b-1}D}\sum_{j=1}^{2^{h-1}Q} a_{i,j}^{r+1}\left[{}_0\mathcal{I}_x^2\psi_i(x)\right]_{x=1}\psi_j(t)\Bigg) \\ & + \sum_{i=1}^{2^{b-1}D}\sum_{j=1}^{2^{h-1}Q} a_{i,j}^{r+1}\left[{}_0\mathcal{I}_x^2\psi_i(x)\right]\psi_j(t).\end{aligned} \tag{4.23}$$

If we substitute equation (4.15), equation (4.22), and equation (4.23) in equation (4.9), and replace $\approx$ by $=$, we get

$$\begin{aligned}&\delta\left[f''(x) + \sum_{i=1}^{2^{b-1}D}\sum_{j=1}^{2^{h-1}Q} a_{i,j}^{r+1}\psi_i(x)\left[{}_0\mathcal{I}_t^\alpha\psi_j(t)\right]\right] \\ &+ (\lambda - \lambda(p+1)y_r^p(x,t))\Bigg[z_1(t) + x\Bigg(z_2(t) - z_1(t) + w(0) + w'(0) - w(1) \\ &- \sum_{i=1}^{2^{b-1}D}\sum_{j=1}^{2^{h-1}Q} a_{i,j}^{r+1}\left[{}_0\mathcal{I}_x^2\psi_i(x)\right]_{x=1}\left[{}_0\mathcal{I}_t^\alpha\psi_j(t)\right]\Bigg) + w(x) - w(0) - xw'(0) \\ &+ \sum_{i=1}^{2^{b-1}D}\sum_{j=1}^{2^{h-1}Q} a_{i,j}^{r+1}\left[{}_0\mathcal{I}_x^2\psi_i(x)\right]\left[{}_0\mathcal{I}_t^\alpha\psi_j(t)\right]\Bigg] + q(x,t) + \lambda p y_r^{p+1}(x,t) \\ &= \left[{}_0^C\mathcal{D}_t^\alpha z_1(t)\right] + x\Bigg(\left[{}_0^C\mathcal{D}_t^\alpha z_2(t)\right] - \left[{}_0^C\mathcal{D}_t^\alpha z_1(t)\right] \\ &- \sum_{i=1}^{2^{b-1}D}\sum_{j=1}^{2^{h-1}Q} a_{i,j}^{r+1}\left[{}_0\mathcal{I}_x^2\psi_i(x)\right]_{x=1}\psi_j(t)\Bigg) + \sum_{i=1}^{2^{b-1}D}\sum_{j=1}^{2^{h-1}Q} a_{i,j}^{r+1}\left[{}_0\mathcal{I}_x^2\psi_i(x)\right]\psi_j(t).\end{aligned} \tag{4.24}$$

If we solve the linear equation (4.24) at the collocation points $x_e = \dfrac{2e-1}{2^bD}$, $t_f = \dfrac{2f-1}{2^hQ}$, where $e = 1, \ldots, 2^{b-1}D$, $f = 1, \ldots, 2^{h-1}Q$, we can obtain the unknown coefficients $a_{i,j}^{r+1}$. We can find an approximate solution by substituting the coefficients $a_{i,j}^{r+1}$ into equation (4.22).

4.3 Convergence Analysis

Theorem 3. [23] Let $y = y(x,t)$ be a square-integrable function on $[0,1) \times [0,1)$, that is $y(x,t) \in L^2([0,1) \times [0,1))$. Suppose that $y(x,t)$ has the property $\left|\frac{\partial^4 y(x,t)}{\partial x^2 \partial t^2}\right| \leq K$, where $K \in \mathbb{R}^+$. Then we have the upper bound

$$|a_{c,d,p,q}| \leq \frac{12K}{c^{5/2}(2d-3)^2\, p^{5/2}(2q-3)^2}, \tag{4.25}$$

for $|a_{c,d,p,q}|$. Moreover, the Legendre wavelets series expansion of $y(x,t)$ converges uniformly to $y(x,t)$.

Proof. Please see [23]. ■

Maleknejad *et al.* [23] gave an upper bound for approximation error when $b = h$ and $D = Q$. Using similar steps, we generalized the upper bound for approximation error. In our error estimation, b need not to be equal h and D need not to be equal Q.

Theorem 4. Let $y = y(x,t)$ be a square-integrable function on $[0,1) \times [0,1)$, that is $y(x,t) \in L^2([0,1) \times [0,1))$. Suppose that $y(x,t)$ has the property $\left|\frac{\partial^4 y(x,t)}{\partial x^2 \partial t^2}\right| \leq K$, where $K \in \mathbb{R}^+$. Then the approximation error can be bounded by the following error estimation

$$\|y(x,t) - y_{b,D,h,Q}(x,t)\|_2 \leq \frac{K}{(2^{b-1})^2(D-1)^{3/2}(2^{h-1})^2(Q-1)^{3/2}}. \tag{4.26}$$

Proof.

$$\|y(x,t) - y_{b,D,h,Q}(x,t)\|_2 = \left(\int_0^1 \int_0^1 \left(y(x,t) - \sum_{c=1}^{2^{b-1}} \sum_{d=0}^{D-1} \sum_{p=1}^{2^{h-1}} \sum_{q=0}^{Q-1} a_{c,d,p,q} \times \psi_{c,d}(x)\psi_{p,q}(t)\right)^2 dx\, dt\right)^{1/2}. \tag{4.27}$$

Note that

$$y(x,t) - \sum_{c=1}^{2^{b-1}} \sum_{d=0}^{D-1} \sum_{p=1}^{2^{h-1}} \sum_{q=0}^{Q-1} a_{c,d,p,q} \psi_{c,d}(x) \psi_{p,q}(t) \tag{4.28}$$

$$= \sum_{c=1}^{\infty} \sum_{d=0}^{\infty} \sum_{p=1}^{\infty} \sum_{q=0}^{\infty} a_{c,d,p,q} \psi_{c,d}(x) \psi_{p,q}(t) - \sum_{c=1}^{2^{b-1}} \sum_{d=0}^{D-1} \sum_{p=1}^{2^{h-1}} \sum_{q=0}^{Q-1} a_{c,d,p,q} \psi_{c,d}(x) \psi_{p,q}(t) \tag{4.29}$$

$$= \sum_{c=2^{b-1}+1}^{\infty} \sum_{d=D}^{\infty} \sum_{p=2^{h-1}+1}^{\infty} \sum_{q=Q}^{\infty} a_{c,d,p,q} \psi_{c,d}(x) \psi_{p,q}(t). \tag{4.30}$$

Thus, it can be stated that

$$\begin{aligned} \|y(x,t) - y_{k,M,h,Q}(x,t)\|_2 = \Bigg(\int_0^1 \int_0^1 \Bigg(\sum_{n=2^{k-1}+1}^{\infty} \sum_{m=M}^{\infty} \sum_{p=2^{h-1}+1}^{\infty} \sum_{q=Q}^{\infty} a_{n,m,p,q} \\ \times \psi_{n,m}(x) \psi_{p,q}(t) \Bigg)^2 dx\, dt \Bigg)^{1/2}. \end{aligned} \tag{4.31}$$

Due to orthonormality (2.15), we have

$$\begin{aligned} \|y(x,t) - y_{b,D,h,Q}(x,t)\|_2 &= \Bigg(\sum_{c=2^{b-1}+1}^{\infty} \sum_{d=D}^{\infty} \sum_{p=2^{h-1}+1}^{\infty} \sum_{q=Q}^{\infty} a_{c,d,p,q}^2 \\ &\quad \times \int_0^1 \int_0^1 \psi_{c,d}^2(x) \psi_{p,q}^2(t)\, dx\, dt \Bigg)^{1/2} \end{aligned} \tag{4.32}$$

$$\begin{aligned} &\leq 12K \Bigg(\sum_{c=2^{b-1}+1}^{\infty} \frac{1}{c^5} \sum_{d=D}^{\infty} \frac{1}{(2d-3)^4} \\ &\quad \times \sum_{p=2^{h-1}+1}^{\infty} \frac{1}{p^5} \sum_{q=Q}^{\infty} \frac{1}{(2q-3)^4} \Bigg)^{1/2}. \end{aligned} \tag{4.33}$$

It is known that

$$\sum_{u=v}^{\infty} \frac{1}{u^w} \leq \frac{1}{(w-1)(v-1)^{(w-1)}}. \tag{4.34}$$

Thus, we have

$$\sum_{c=2^{b-1}+1}^{\infty} \frac{1}{c^5} \leq \frac{1}{4(2^{b-1})^4}, \tag{4.35}$$

$$\sum_{p=2^{h-1}+1}^{\infty} \frac{1}{p^5} \leq \frac{1}{4(2^{h-1})^4}. \tag{4.36}$$

Note that

$$\sum_{d=D}^{\infty} \frac{1}{(2d-3)^4} \leq \sum_{d=D}^{\infty} \frac{1}{d^4}, \qquad \text{for } d \geq 3, \tag{4.37}$$

$$\sum_{q=Q}^{\infty} \frac{1}{(2q-3)^4} \leq \sum_{q=Q}^{\infty} \frac{1}{q^4}, \qquad \text{for } q \geq 3. \tag{4.38}$$

Therefore, we can write

$$\sum_{d=D}^{\infty} \frac{1}{(2d-3)^4} \leq \frac{1}{3(D-1)^3}, \tag{4.39}$$

$$\sum_{q=Q}^{\infty} \frac{1}{(2q-3)^4} \leq \frac{1}{3(Q-1)^3}. \tag{4.40}$$

As a result, we conclude that

$$\begin{aligned} \|y(x,t) - y_{b,D,h,Q}(x,t)\|_2 \leq 12K \Bigg(& \sum_{c=2^{b-1}+1}^{\infty} \frac{1}{c^5} \sum_{d=D}^{\infty} \frac{1}{(2d-3)^4} \\ & \times \sum_{p=2^{h-1}+1}^{\infty} \frac{1}{p^5} \sum_{q=Q}^{\infty} \frac{1}{(2q-3)^4} \Bigg)^{1/2} \end{aligned} \tag{4.41}$$

$$\leq \frac{K}{(2^{b-1})^2 (D-1)^{3/2} (2^{h-1})^2 (Q-1)^{3/2}}. \tag{4.42}$$

This completes the proof. ■

4.4 Numerical Examples

We will solve some test problems to investigate the effectiveness of the Legendre wavelet collocation method with quasilinearization technique (LWCMQT). In addition, maximum absolute errors

$$E_{L_\infty} := \max |y_{exact}(x_e, t_f) - y_{approximate}(x_e, t_f)| \tag{4.43}$$

where the maximum is taken over all collocation points (x_e, t_f), will be compared with the Haar wavelet collocation iteration method (HWCIM) [2] and the modified variational iteration method (MVIM) [28]. In all examples, we will take the resolution levels $b = 2$, $h = 2$ and $D = 2$, $Q = 2$ and iterate the quasilinearization technique three times. All calculations and graphs were obtained using Wolfram Mathematica Online [16].

Example 4.1. In the first test problem, we solve the following time-fractional homogeneous Fisher's equation

$$\frac{\partial^\alpha y(x,t)}{\partial t^\alpha} = \frac{\partial^2 y(x,t)}{\partial x^2} + y(x,t)\left(1 - y^6(x,t)\right), \tag{4.44}$$

with the initial condition

$$y(x,0) = \left(1 + e^{\frac{3x}{2}}\right)^{-\frac{1}{3}}, \tag{4.45}$$

and boundary conditions

$$y(0,t) = \left(1 + e^{\frac{-15t}{4}}\right)^{-\frac{1}{3}}, \tag{4.46}$$

$$y(1,t) = \left(1 + e^{\frac{6-15t}{4}}\right)^{-\frac{1}{3}}. \tag{4.47}$$

The exact solution for $\alpha = 1$ is

$$y_{exact}(x,t) = \left(1 + e^{\frac{6x-15t}{4}}\right)^{-\frac{1}{3}}. \tag{4.48}$$

We use $y_0(x,t) = \left(1 + e^{\frac{3x}{2}}\right)^{-\frac{1}{3}}$ as an initial guess and implement the Legendre wavelet collocation method with quasilinearization technique. We iterate the quasilinearization technique three times. In Table 4.1, the numerical results for the resolution levels $b = 2$, $h = 2$ and the degree of polynomials $D = 2, Q = 2$ are presented. The maximum absolute errors of some other methods are compared in Table 4.2. The approximate solution is plotted in Figure 4.1. Also, the absolute error is illustrated in Figure 4.2.

Figure 4.1. Numerical solution for $\alpha = 1$ obtained by LWCMQT with $b = 2$, $h = 2$ and $D = 2, Q = 2$ in the 3^{rd} iteration in Example 4.1

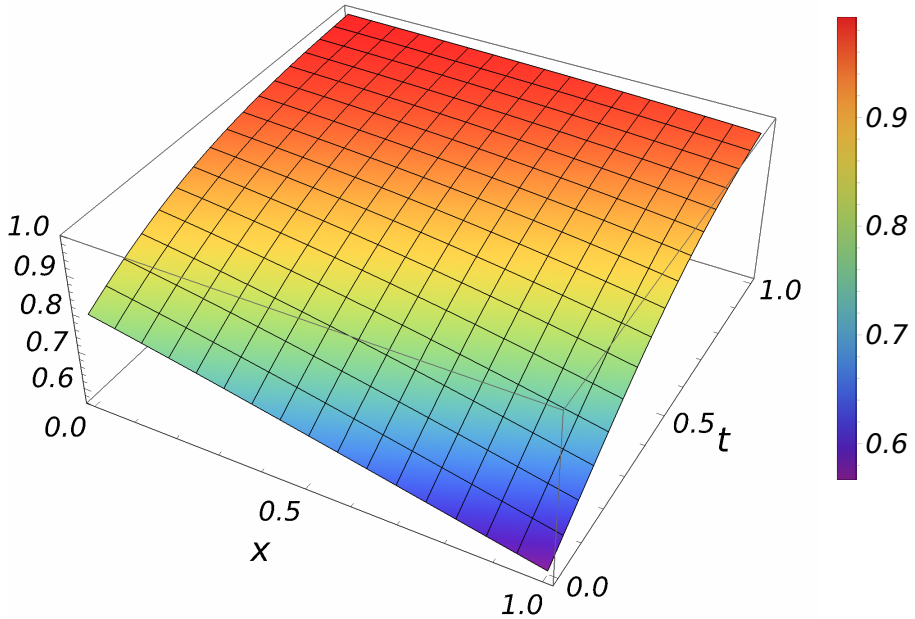

Table 4.1. Numerical results for Example 4.1 obtained by using the LWCMQT with the resolution levels $b = 2$, $h = 2$ and the degree of polynomials $D = 2$, $Q = 2$

Col. Pts. (x,t)	$\alpha = 0.5$ $y_3(x,t)$	$\alpha = 0.7$ $y_3(x,t)$	$\alpha = 0.9$ $y_3(x,t)$	$\alpha = 1$ $y_3(x,t)$	Absolute error for $\alpha = 1$ $\lvert y_{exact}(x,t) - y_3(x,t)\rvert$
$(\frac{1}{8}, \frac{1}{8})$	0.841965	0.837217	0.831816	0.829149	$8.64386E-05$
$(\frac{1}{8}, \frac{3}{8})$	0.920330	0.919341	0.918173	0.917268	$2.83358E-05$
$(\frac{1}{8}, \frac{5}{8})$	0.960751	0.961107	0.962609	0.964099	$4.83664E-05$
$(\frac{1}{8}, \frac{7}{8})$	0.980168	0.981730	0.983990	0.985399	$6.85387E-05$
$(\frac{3}{8}, \frac{1}{8})$	0.809699	0.799151	0.787212	0.781343	$2.34064E-04$
$(\frac{3}{8}, \frac{3}{8})$	0.895346	0.893036	0.889976	0.887503	$8.54197E-05$
$(\frac{3}{8}, \frac{5}{8})$	0.942496	0.943067	0.946154	0.949353	$8.42780E-05$
$(\frac{3}{8}, \frac{7}{8})$	0.967799	0.971121	0.975982	0.979079	$1.44718E-04$
$(\frac{5}{8}, \frac{1}{8})$	0.757606	0.746537	0.733928	0.727673	$2.50099E-04$
$(\frac{5}{8}, \frac{3}{8})$	0.859489	0.856715	0.853110	0.850308	$1.36321E-04$
$(\frac{5}{8}, \frac{5}{8})$	0.922621	0.923055	0.926167	0.929488	$5.55606E-05$
$(\frac{5}{8}, \frac{7}{8})$	0.957987	0.961485	0.966695	0.970038	$1.22053E-04$
$(\frac{7}{8}, \frac{1}{8})$	0.685000	0.679575	0.673283	0.670091	$1.03955E-04$
$(\frac{7}{8}, \frac{3}{8})$	0.810705	0.809069	0.807159	0.805823	$8.18697E-05$
$(\frac{7}{8}, \frac{5}{8})$	0.900009	0.900163	0.901686	0.903333	$1.13899E-05$
$(\frac{7}{8}, \frac{7}{8})$	0.951098	0.952903	0.955655	0.957412	$4.45979E-05$

Table 4.2. Maximum absolute errors (E_{L_∞}) of LWCMQT, HWCIM [2], and MVIM [28] for the numerical solution of Example 4.1

The Method	Maximum Absolute Error (E_{L_∞})
LWCMQT	$2.50099E-04$
HWCIM	$1.17E-03$
MVIM	$1.97465E-01$

Figure 4.2. The absolute error $|y_{exact}(x,t) - y_3(x,t)|$ of Example 4.1

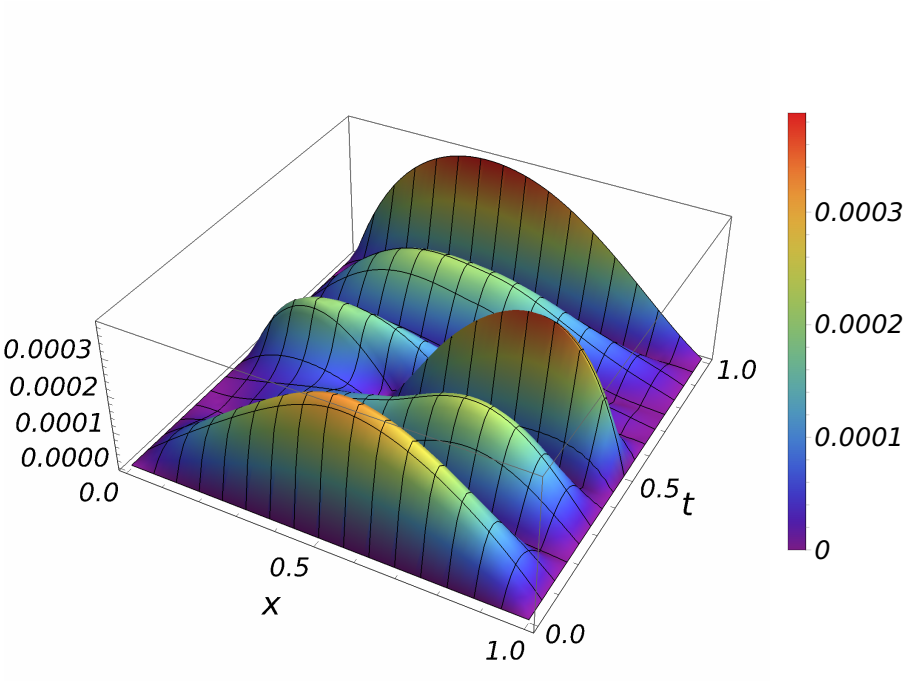

Example 4.2. In the second example, we consider the following time-fractional homogeneous Fisher's equation

$$\frac{\partial^\alpha y(x,t)}{\partial t^\alpha} = \frac{\partial^2 y(x,t)}{\partial x^2} + y(x,t)\left(1 - y(x,t)\right), \tag{4.49}$$

with the initial condition

$$y(x,0) = \mu, \tag{4.50}$$

and boundary conditions

$$y(0,t) = \frac{\mu e^t}{1 - \mu + \mu e^t}, \tag{4.51}$$

$$y(1,t) = \frac{\mu e^t}{1 - \mu + \mu e^t}, \tag{4.52}$$

where μ is a constant. The exact solution for $\alpha = 1$ is given by

$$y_{exact}(x,t) = \frac{\mu e^t}{1-\mu+\mu e^t}. \tag{4.53}$$

We use $y_0(x,t) = \mu$ as an initial guess and implement the Legendre wavelet collocation method with quasilinearization technique. We iterate the quasilinearization technique three times. In Table 4.3, the numerical results for $\mu = \frac{2}{3}$, $b = 2$, $h = 2$ and $D = 2$, $Q = 2$ are presented. The maximum absolute errors of some other methods are compared in Table 4.4. The approximate solution is plotted in Figure 4.3. Also, the absolute error is illustrated in Figure 4.4.

Figure 4.3. Numerical solution for $\mu = \frac{2}{3}$ and $\alpha = 1$ obtained by LWCMQT with $b = 2$, $h = 2$ and $D = 2$, $Q = 2$ in the 3^{rd} iteration in Example 4.2

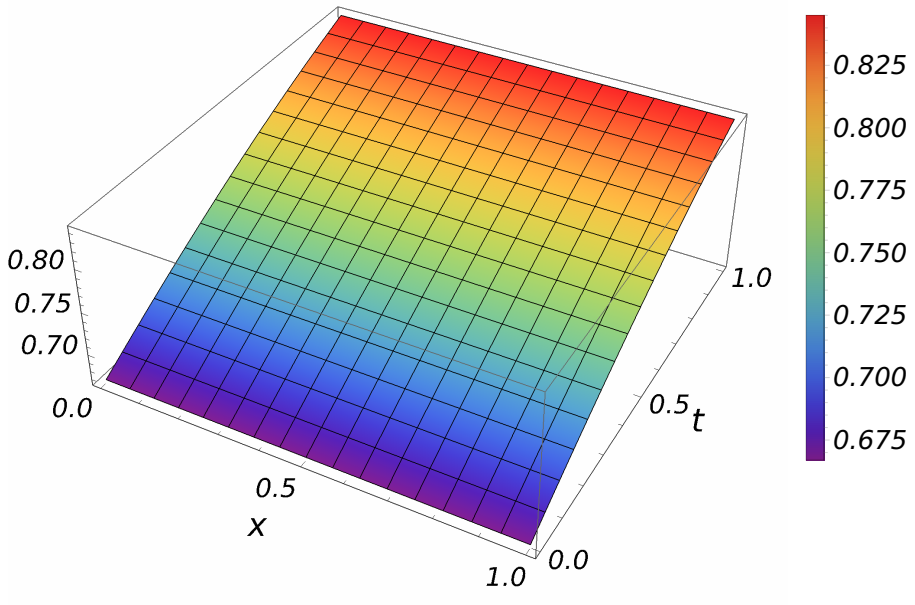

Table 4.3. Numerical results for Example 4.2 obtained by using the LWCMQT with the resolution levels $b = 2$, $h = 2$ and the degree of polynomials $D = 2$, $Q = 2$

Col. Pts. (x,t)	$\alpha = 0.5$ $y_3(x,t)$	$\alpha = 0.7$ $y_3(x,t)$	$\alpha = 0.9$ $y_3(x,t)$	$\alpha = 1$ $y_3(x,t)$	Absolute error for $\alpha = 1$ $\lvert y_{exact}(x,t) - y_3(x,t)\rvert$
$(\frac{1}{8}, \frac{1}{8})$	0.699479	0.697388	0.695016	0.693843	$0.00000E-00$
$(\frac{1}{8}, \frac{3}{8})$	0.747179	0.746198	0.745017	0.744244	$0.00000E-00$
$(\frac{1}{8}, \frac{5}{8})$	0.789141	0.788652	0.788610	0.788873	$1.11022E-16$
$(\frac{1}{8}, \frac{7}{8})$	0.826046	0.826320	0.826995	0.827519	$2.88658E-15$
$(\frac{3}{8}, \frac{1}{8})$	0.705598	0.701172	0.696237	0.693843	$0.00000E-00$
$(\frac{3}{8}, \frac{3}{8})$	0.750559	0.748549	0.745995	0.744244	$0.00000E-00$
$(\frac{3}{8}, \frac{5}{8})$	0.789508	0.788461	0.788339	0.788873	$4.44089E-16$
$(\frac{3}{8}, \frac{7}{8})$	0.824498	0.825061	0.826431	0.827519	$7.77156E-15$
$(\frac{5}{8}, \frac{1}{8})$	0.705598	0.701172	0.696237	0.693843	$0.00000E-00$
$(\frac{5}{8}, \frac{3}{8})$	0.750559	0.748549	0.745995	0.744244	$0.00000E-00$
$(\frac{5}{8}, \frac{5}{8})$	0.789508	0.788461	0.788339	0.788873	$2.22045E-16$
$(\frac{5}{8}, \frac{7}{8})$	0.824498	0.825061	0.826431	0.827519	$7.99361E-15$
$(\frac{7}{8}, \frac{1}{8})$	0.699479	0.697388	0.695016	0.693843	$0.00000E-00$
$(\frac{7}{8}, \frac{3}{8})$	0.747179	0.746198	0.745017	0.744244	$0.00000E-00$
$(\frac{7}{8}, \frac{5}{8})$	0.789141	0.788652	0.788610	0.788873	$2.22045E-16$
$(\frac{7}{8}, \frac{7}{8})$	0.826046	0.826320	0.826995	0.827519	$2.88658E-15$

Table 4.4. Maximum absolute errors (E_{L_∞}) of LWCMQT, HWCIM [2], and MVIM [28] for the numerical solution of Example 4.2

The Method	Maximum Absolute Error (E_{L_∞})
LWCMQT	$7.99361E-15$
HWCIM	$2.19E-05$
MVIM	$3.68E-02$

Figure 4.4. The absolute error $|y_{exact}(x,t) - y_3(x,t)|$ of Example 4.2

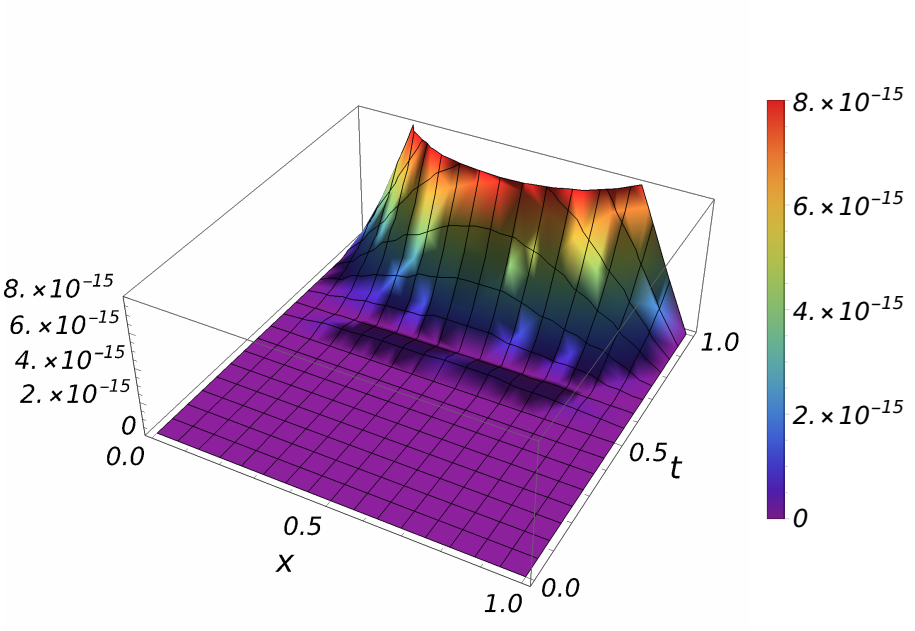

Example 4.3. In the third test problem, we solve the following time-fractional non-homogeneous Fisher's equation

$$\frac{\partial^\alpha y(x,t)}{\partial t^\alpha} = \frac{\partial^2 y(x,t)}{\partial x^2} + y(x,t)\left(1 - y^3(x,t)\right) + q(x,t), \tag{4.54}$$

where

$$q(x,t) = t\left(-2 - x(t+x)\left(1 - t^3x^3(t+x)^3\right) + \frac{x^2t^{-\alpha}}{\Gamma(2-\alpha)} + \frac{2xt^{1-\alpha}}{\Gamma(3-\alpha)}\right), \tag{4.55}$$

with the initial condition

$$y(x,0) = 0, \tag{4.56}$$

and boundary conditions

$$y(0,t) = 0, \tag{4.57}$$

$$y(1,t) = t^2 + t. \tag{4.58}$$

When $\alpha = 1$, the problem has the exact solution

$$y_{exact}(x,t) = xt^2 + tx^2. \tag{4.59}$$

We use $y_0(x,t) = 0$ as an initial guess and implement the Legendre wavelet collocation method with quasilinearization technique. We iterate the quasilinearization technique three times. In Table 4.5, the numerical results for the resolution levels $b = 2$, $h = 2$ and the degree of polynomials $D = 2$, $Q = 2$ are presented. The maximum absolute errors of some other methods are compared in Table 4.6. The approximate solution is plotted in Figure 4.5. Also, the absolute error is illustrated in Figure 4.6.

Figure 4.5. Numerical solution for $\alpha = 1$ obtained by LWCMQT with $b = 2$, $h = 2$ and $D = 2$, $Q = 2$ in the 3^{rd} iteration in Example 4.3

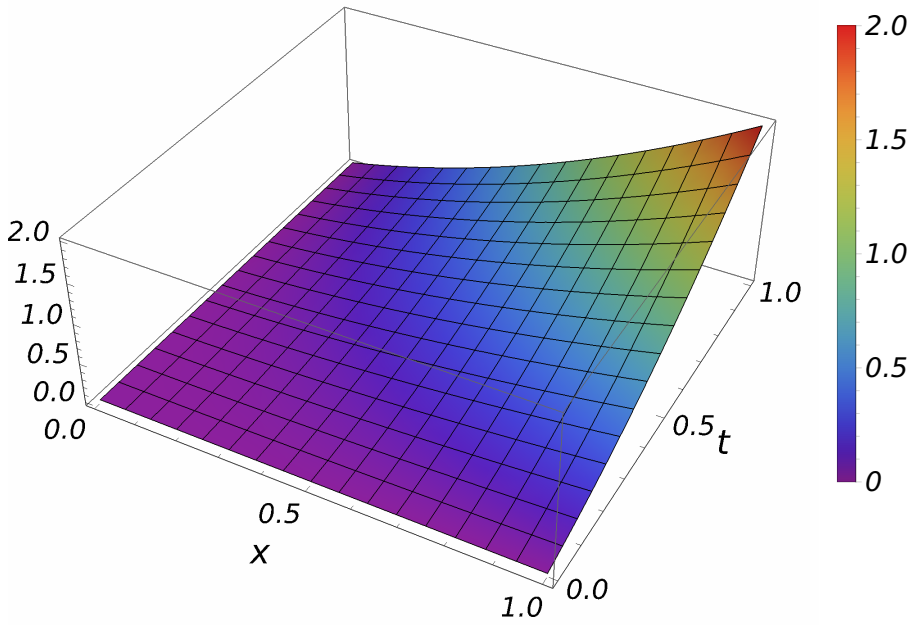

Table 4.5. Numerical results for Example 4.3 obtained by using the Legendre wavelet collocation method with quasilinearization technique with the resolution levels $b = 2$, $h = 2$ and the degree of polynomials $D = 2,\ \ Q = 2$

Col. Pts. (x,t)	$\alpha = 0.5$ $y_3(x,t)$	$\alpha = 0.7$ $y_3(x,t)$	$\alpha = 0.9$ $y_3(x,t)$	$\alpha = 1$ $y_3(x,t)$	Absolute error for $\alpha = 1$ $\lvert y_{exact}(x,t) - y_3(x,t)\rvert$
$(\frac{1}{8}, \frac{1}{8})$	0.003635	0.003507	0.003635	0.003906	$8.67362E-19$
$(\frac{1}{8}, \frac{3}{8})$	0.023602	0.023678	0.023568	0.023437	$6.93889E-18$
$(\frac{1}{8}, \frac{5}{8})$	0.058457	0.058386	0.058470	0.058593	$2.29585E-09$
$(\frac{1}{8}, \frac{7}{8})$	0.109399	0.109417	0.109399	0.109375	$1.30438E-08$
$(\frac{3}{8}, \frac{1}{8})$	0.022788	0.022480	0.022788	0.023437	$6.93889E-18$
$(\frac{3}{8}, \frac{3}{8})$	0.105861	0.106040	0.105776	0.105469	$0.00000E-00$
$(\frac{3}{8}, \frac{5}{8})$	0.234052	0.233886	0.234089	0.234375	$6.16237E-09$
$(\frac{3}{8}, \frac{7}{8})$	0.410211	0.410251	0.410205	0.410156	$4.49039E-08$
$(\frac{5}{8}, \frac{1}{8})$	0.057944	0.057637	0.057944	0.058593	$6.93889E-18$
$(\frac{5}{8}, \frac{3}{8})$	0.234767	0.234946	0.234681	0.234375	$5.55112E-17$
$(\frac{5}{8}, \frac{5}{8})$	0.487962	0.487799	0.487999	0.488281	$7.27352E-09$
$(\frac{5}{8}, \frac{7}{8})$	0.820365	0.820403	0.820359	0.820313	$8.52705E-08$
$(\frac{7}{8}, \frac{1}{8})$	0.109105	0.108976	0.109104	0.109375	$1.38779E-17$
$(\frac{7}{8}, \frac{3}{8})$	0.410320	0.410396	0.410287	0.410156	$1.11022E-16$
$(\frac{7}{8}, \frac{5}{8})$	0.820182	0.820114	0.820194	0.820312	$3.49513E-09$
$(\frac{7}{8}, \frac{7}{8})$	1.339860	1.339880	1.339870	1.339840	$6.49032E-08$

Table 4.6. Maximum absolute errors (E_{L_∞}) of LWCMQT, and HWCIM [2] for the numerical solution of Example 4.3

The Method	Maximum Absolute Error (E_{L_∞})
LWCMQT	$8.52705E-08$
HWCIM	$1.19E-03$

Figure 4.6. The absolute error $|y_{exact}(x,t) - y_3(x,t)|$ of Example 4.3

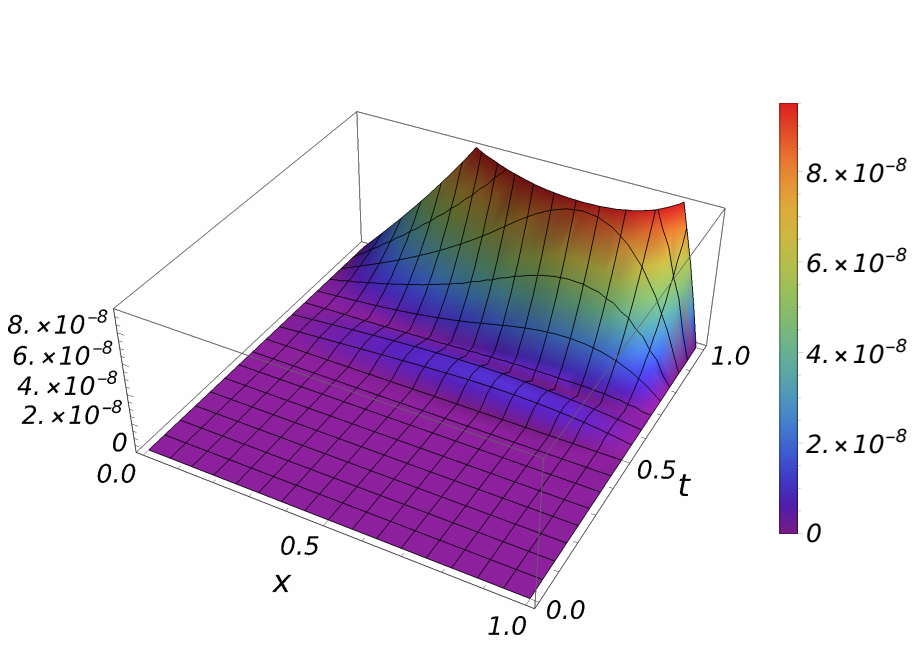

CHAPTER 5

CONCLUSION

In this thesis, our main goal was to develop efficient numerical methods based on Legendre wavelets and quasilinearization technique for fractional Lane-Emden type equation (1.3) and the time-fractional Fisher's equation (1.5).

In Chapter 1, we briefly explained why we study fractional differential equations and why we use wavelets for numerical solution of differential equations.

Chapter 2 consists of the basic definitions and properties of fractional calculus and Legendre wavelets. Additionally, we gave a formula for the Riemann-Liouville integral of Legendre wavelets in Chapter 2.

We started Chapter 3 by explaining quasilinearization technique for fractional Lane-Emden type equation (1.3) in detail. Then we developed our method based on Legendre wavelets and quasilinearization technique for fractional Lane-Emden type equation (1.3). We solved three examples to assess the efficiency of the presented method for fractional Lane-Emden type equations (1.3). Numerical results support that the presented method for fractional Lane-Emden type equations (1.3) performs better than Haar Wavelet Collocation Method (HWCM) [34], Haar Wavelet Collocation Adomian Method (HWCAM) [32], and Adomian Decomposition Method (ADM) [42]. In many cases, the proposed method for fractional Lane-Emden type equations (1.3) yields better results than Chebyshev Wavelet Collocation Quasilinearization Method (CWCQM) [27]. However, Chebyshev Wavelet Collocation Quasilinearization Method (CWCQM) [27] produced slightly better results in some situations. As a result, both Chebyshev Wavelet Collocation Quasilinearization Method (CWCQM) [27] and the proposed method for fractional Lane-Emden type equations (1.3) give satisfactory results and either of these two methods can be used to get very accurate approximate solutions for fractional Lane-Emden type equations (1.3).

In Chapter 4, we described quasilinearization technique for the time-fractional Fisher's equation (1.5) in depth. Then we derived our method utilizing Legendre wavelets

and quasilinearization technique for the time-fractional Fisher's equation (1.5). To investigate the efficiency of the proposed method for the time-fractional Fisher's equation (1.5), three numerical examples were solved. The examples show that the proposed method is quite effective even when the resolution levels b, h and the degree of polynomials D, Q are very small.

There are two new theoretical contributions to the literature in this thesis. Theorem 1 is the first theoretical contribution and it is useful for fast computation of the Riemann-Liouville integral of Legendre wavelets on a computer. The second theoretical contribution is Theorem 4. We gave an upper bound for the approximation error in Theorem 4.

We first iteratively linearized the fractional Lane-Emden type equation and the time-fractional Fisher equation. We then developed numerical methods based on Legendre wavelets for these two equations. Anyone interested in this topic can develop numerical methods based on Legendre wavelets without linearizing the fractional Lane-Emden type equation and the time-fractional Fisher equation. Then, the resulting system of algebraic equations can be solved using Newton's method and the numerical results can be compared with the numerical results in this thesis.

We used 2-scale Legendre wavelets and performed convergence analysis for 2-scale Legendre wavelets. It is also possible to define Legendre wavelets different than 2-scale Legendre wavelets such as 3-scale Legendre wavelets, 4-scale Legendre wavelets, etc. We predict that 3-scale Legendre wavelets and 4-scale Legendre wavelets will yield more accurate numerical results than 2-scale Legendre wavelets. As far as we know, there is no research on this topic. A research can be conducted on this subject.

REFERENCES

[1] N. Aghazadeh, A. Mohammadi, and G. Tanoglu. Taylor wavelets collocation technique for solving fractional nonlinear singular pdes. *Mathematical Sciences*, 2022.

[2] G. Ahmadnezhad, N. Aghazadeh, and S. Rezapour. Haar wavelet iteration method for solving time fractional fisher's equation. *Computational Methods for Differential Equations*, 8(3):505–522, 2020.

[3] T. Atanackovic, S. Pilipovic, B. Stanković, and D. Zorica. *Fractional Calculus with Applications in Mechanics: Vibrations and Diffusion Processes*. John Wiley & Sons, 01 2014.

[4] R. E. Bellman and R. E. Kalaba. *Quasilinearization and nonlinear boundary-value problems*. RAND Corporation, Santa Monica, CA, 1965.

[5] M. D. Bramson. Maximal displacement of branching brownian motion. *Communications on Pure and Applied Mathematics*, 31(5):531–581, 1978.

[6] S. Chandrasekhar. *An Introduction to the Study of Stellar Structure*. Dover Publications, 2010.

[7] G. cheng Wu. A fractional variational iteration method for solving fractional nonlinear differential equations. *Computers & Mathematics with Applications*, 61(8):2186–2190, 2011. Advances in Nonlinear Dynamics.

[8] L. C. de Barros, M. M. Lopes, F. S. Pedro, E. Esmi, J. P. C. dos Santos, and D. E. Sánchez. The memory effect on fractional calculus: an application in the spread of covid-19. *Computational and Applied Mathematics*, 40(72), 2021.

[9] L. Debnath. Recent applications of fractional calculus to science and engineering. *International Journal of Mathematics and Mathematical Sciences*, 2003(54):3413–3442, 2003.

[10] M. Faheem, A. Khan, and A. Raza. A high resolution hermite wavelet technique for solving space–time-fractional partial differential equations. *Mathematics and Computers in Simulation*, 194:588–609, 2022.

[11] R. A. Fisher. The wave of advance of advantageous genes. *Annals of Eugenics*, 7(4):355–369, 1937.

[12] Y. Gouari, Z. Dahmani, S. E. Farooq, and F. Ahmad. Fractional singular differential systems of lane–emden type: Existence and uniqueness of solutions. *Axioms*, 9(3), 2020.

[13] S. Gümgüm. Taylor wavelet solution of linear and nonlinear lane-emden equations. *Applied Numerical Mathematics*, 158:44–53, 2020.

[14] Z. Hao and Z. Zhang. Fast spectral petrov-galerkin method for fractional elliptic equations. *Applied Numerical Mathematics*, 162:318–330, 2021.

[15] R. Hilfer. *Applications of Fractional Calculus in Physics*. World Scientific, 2000.

[16] W. R. Inc. Mathematica, Version 13.1. Champaign, IL, 2022.

[17] H. Jafari and V. Daftardar-Gejji. Solving a system of nonlinear fractional differential equations using adomian decomposition. *Journal of Computational and Applied Mathematics*, 196(2):644–651, 2006.

[18] B. Jin. *Fractional differential equations: An approach via fractional derivatives*, volume 206 of *Applied Mathematical Sciences*. Springer, 2021.

[19] V. Kenkre. Results from variants of the Fisher equation in the study of epidemics and bacteria. *Physica A: Statistical Mechanics and its Applications*, 342(1):242–248, 2004.

[20] H. Kim, K. H. Kim, and B. Jang. Shifted jacobi spectral-galerkin method for solving fractional order initial value problems. *Journal of Computational and Applied Mathematics*, 380:112988, 2020.

[21] C. Li and F. Zeng. The finite difference methods for fractional ordinary differential equations. *Numerical Functional Analysis and Optimization*, 34(2):149–179, 2013.

[22] J. A. T. Machado, M. F. Silva, R. S. Barbosa, I. S. Jesus, C. M. Reis, M. G. Marcos, and A. F. Galhano. Some Applications of Fractional Calculus in Engineering. *Mathematical Problems in Engineering*, 2010:1–34, 2010.

[23] K. Maleknejad and A. Hoseingholipour. The impact of legendre wavelet collocation method on the solutions of nonlinear system of two-dimensional integral equations. *International Journal of Computer Mathematics*, 97(11):2287–2302, 2020.

[24] V. B. Mandelzweig. Quasilinearization method and its verification on exactly solvable models in quantum mechanics. *Journal of Mathematical Physics*, 40(12):6266–6291, 1999.

[25] W. S. Marco Gallegati. *Wavelet Applications in Economics and Finance*. Dynamic Modeling and Econometrics in Economics and Finance. Springer, 2014.

[26] M. Mehra. *Applications of Wavelet in Inverse Problems*. Springer Singapore, Singapore, 2018.

[27] A. Mohammadi, G. Ahmadnezhad, and N. Aghazadeh. Chebyshev quasilinearization method for solving fractional singular nonlinear Lane-Emden equations. *Communications in Mathematics*, Volume 30 (2022), Issue 1, Sept. 2022.

[28] S. T. Mohyud-Din and M. A. Noor. Modified variational iteration method for solving fisher's equations. *Journal of Applied Mathematics and Computing*, 31:295–308, 2009.

[29] S. Momani and Z. Odibat. Analytical approach to linear fractional partial differential equations arising in fluid mechanics. *Physics Letters A*, 355(4):271–279, 2006.

[30] K. Parand, M. Dehghan, A. Rezaei, and S. Ghaderi. An approximation algorithm for the solution of the nonlinear lane–emden type equations arising in astrophysics using hermite functions collocation method. *Computer Physics Communications*, 181(6):1096–1108, 2010.

[31] J. Ross, A. F. Villaverde, J. R. Banga, S. Vázquez, and F. Morán. A generalized fisher equation and its utility in chemical kinetics. *Proceedings of the National Academy of Sciences*, 107(29):12777–12781, 2010.

[32] U. Saeed. Haar Adomian Method for the Solution of Fractional Nonlinear Lane-Emden Type Equations Arising in Astrophysics. *Taiwanese Journal of Mathematics*, 21(5):1175 – 1192, 2017.

[33] A. Secer and M. Cinar. A jacobi wavelet collocation method for fractional fisher's equation in time. *Thermal Science*, 24:119–129, 2020.

[34] S. Shiralashetti, A. Deshi, and P. Mutalik Desai. Haar wavelet collocation method for the numerical solution of singular initial value problems. *Ain Shams Engineering Journal*, 7(2):663–670, 2016.

[35] R. Singh, H. Garg, and V. Guleria. Haar wavelet collocation method for lane–emden equations with dirichlet, neumann and neumann–robin boundary conditions. *Journal of Computational and Applied Mathematics*, 346:150–161, 2019.

[36] H. Srivastava, K. M. Saad, and M. Khader. An efficient spectral collocation method for the dynamic simulation of the fractional epidemiological model of the ebola virus. *Chaos, Solitons & Fractals*, 140:110174, 2020.

[37] A. Teolis. *Computational Signal Processing with Wavelets*. Applied and Numerical Harmonic Analysis. Springer, 1998.

[38] P. J. Torvik and R. L. Bagley. On the Appearance of the Fractional Derivative in the Behavior of Real Materials. *Journal of Applied Mechanics*, 51(2):294–298, 06 1984.

[39] L. Wang, Y. Ma, and Z. Meng. Haar wavelet method for solving fractional partial differential equations numerically. *Applied Mathematics and Computation*, 227:66–76, 2014.

[40] Q. Wang. Homotopy perturbation method for fractional kdv-burgers equation. *Chaos, Solitons & Fractals*, 35(5):843–850, 2008.

[41] Y. Wang and Q. Fan. The second kind chebyshev wavelet method for solving fractional differential equations. *Applied Mathematics and Computation*, 218(17):8592–8601, 2012.

[42] A.-M. Wazwaz. Adomian decomposition method for a reliable treatment of the emden–fowler equation. *Applied Mathematics and Computation*, 161(2):543–560, 2005.

[43] B. Yuttanan and M. Razzaghi. Legendre wavelets approach for numerical solutions of distributed order fractional differential equations. *Applied Mathematical Modelling*, 70:350–364, 2019.

[44] B. Yuttanan, M. Razzaghi, and T. N. Vo. Legendre wavelet method for fractional delay differential equations. *Applied Numerical Mathematics*, 168:127–142, 2021.

[45] M. Zayernouri and G. E. Karniadakis. Fractional spectral collocation methods for linear and nonlinear variable order fpdes. *Journal of Computational Physics*, 293:312–338, 2015. Fractional PDEs.